Bidding Strategy for Networked Microgrids in the Day-Ahead Electricity Market

A Thesis Submitted to the

College of Graduate and Postdoctoral Studies

In Partial Fulfillment of the Requirements

For the Degree of Master of Science

In the Department of Electrical and Computer Engineering

University of Saskatchewan

Saskatoon, SK, Canada

By

Bo Hu

Permission to Use

In presenting this thesis in partial fulfillment of the requirements for a Postgraduate degree from the University of Saskatchewan, I agree that the Libraries of this University may make it freely available for inspection. I further agree that permission for copying of this thesis in any manner, in whole or in part, for scholarly purposes may be granted by the professor or professors who supervised my thesis/dissertation work or, in their absence, by the Head of the Department or the Dean of the College in which my thesis work was done. It is understood that any copying or publication or use of this thesis or parts thereof for financial gain shall not be allowed without my written permission. It is also understood that due recognition shall be given to me and to the University of Saskatchewan in any scholarly use which may be made of any material in my thesis.

Requests of permission to copy or to make other uses of materials in this thesis in whole or part should be addressed to:

Head of the Department of Electrical and Computer Engineering
57 Campus Drive
University of Saskatchewan
Saskatoon, Saskatchewan, S7N 5A9
Canada

OR

Dean
College of Graduate and Postdoctoral Studies
University of Saskatchewan
116 Thorvaldson Building, 110 Science Place
Saskatoon, Saskatchewan S7N 5C9
Canada

Abstract

In recent years, microgrids have drawn increasing attention from both academic and industrial sectors due to their enormous potential benefits to the power systems. Microgrids are essentially highly-customized small-scale power systems. Microgrids' islanding capability enables microgrids to conduct more flexible and energy-efficient operations. Microgrids have proved to be able to provide reliable and environmental-friendly electricity to quality-sensitive or off-grid consumers. In addition, during the grid-connected operation mode, microgrids can also provide support to the utility grid. World-widely continuous microgrid deployments indicate a paradigm shift from traditional centralized large-scale systems toward more distributed and customized small-scale systems. However, microgrids can cause as many problems as it solves. More efforts are needed to address these problems caused by microgrids integration. Considering there will be multiple microgrids in future power systems, the coordination problems between individual microgrids remain to be solved. Aiming at facilitating the promotion of microgrids, this thesis investigates the system-level modeling methods for coordination between multiple microgrids in the context of participating in the market. Firstly, this thesis reviews the background and recent development of microgrid coordination models. Problems of existing studies are identified. Motivated by these problems, the research objectives and structure of this thesis are presented. Secondly, this thesis examines and compares the most common frameworks for optimization under uncertainty. An improved unit commitment model considering uncertain sub-hour wind power ramp behaviors is presented to illustrate the reformulation and solution method of optimization models with uncertainty. Next, the price-maker bidding strategy for collaborative networked microgrids is presented. Multiple microgrids are coordinated as a single dispatchable entity and participate in the market as a price-maker. The market-clearing process is modeled using system residual supply/demand price-quota curves. Multiple uncertainty sources in the bidding model are mitigated with a hybrid stochastic-robust optimization framework. What's more, this thesis further considers the privacy concerns of individual microgrids in the coordination process. Therefore a privacy-preserving solution method based on Dantzig-Wolfe decomposition is proposed to solve the bidding problem. Both computational and economic performances of the proposed model are compared with the performances of conventional centralized coordination framework. Lastly, this

thesis provides suggestions on future research directions of coordination problems among multiple microgrids.

Acknowledgments

First of all, I would like to thank my supervisor, Prof. C. Y. Chung, for his guidance, patience, and support during my master study. His breadth of knowledge and expertise were crucial to the completion of this thesis.

I would like to thank all members of Smart Grid and Renewable Energy Technology Lab, for their efforts in creating a motivating working environment. In particular, I would like to thank Dr. Yuzhong Gong, Dr. Weijia Liu, Mr. Yuchuan Chen, Mr. Peiyan Li Mr. Bingzhi Wang, and Mr. Osama Ansari, for their suggestions and assistance to this thesis.

I would also like to thank the NSERC/SaskPower Senior Industrial Research Chair Program, the University of Saskatchewan and the Government of Saskatchewan, for providing financial support during my master study.

Last but not least, I would like to thank my parents, for their readily support and unconditional love. I would not have accomplished this achievement without them.

Thank you all for your support!

Table of Contents

Permission to Use i

Abstract ii

Acknowledgments iv

Table of Contents v

List of Figures viii

List of Tables ix

List of Abbreviations x

1 Introduction 1

1.1 Background 1

1.2 Development of Microgrids 4

1.2.1 Configurations of Microgrids 4

1.2.2 Benefits of Microgrids 5

1.2.3 Current Studies on Microgrids 6

1.3 Problems Statement 8

1.3.1 Price-Maker Bidding Strategy 8

1.3.2 Optimization Method 8

1.3.3 Coordination Framework for Microgrids 8

1.4 Research Objectives 8

1.5 Thesis Outline 9

2 Optimization under Uncertainty 11

2.1 Abstract 11

2.2 Nomenclature 11

2.3 Introduction 13
2.3.1 Stochastic Optimization Methods 13
2.3.2 Robust Optimization Methods 15
2.3.3 Other Methods 17
2.4 Flexible Robust DAUC Model 17
2.5 Background 19
2.6 Model Formulation 20
2.6.1 Analysis of the Sub-hourly Wind Power Ramp Behaviors 20
2.6.2 Improved 2-Stage Robust DAUC Model Considering Sub-Hourly Wind Power Ramp Behaviors 21
2.7 C&CG-based Solution Methodology 25
2.8 Case Study 26
2.8.1 Sub-hourly Wind Power Ramp Behaviors. 26
2.8.2 Flexible UC Decisions 28
2.9 Conclusion 30
3 Price-Maker Bidding Model for Networked Microgrids under Uncertainty 31
3.1 Abstract 31
3.2 Nomenclature 31
3.3 Introduction 35
3.4 Modeling Approach 37
3.5 Model Formulation 41
3.5.1 Controllable Generators Constraints 41
3.5.2 Energy Storage Systems Constraints 42
3.5.3 Deferrable Loads Constraints 42
3.5.4 Transmission Capacity Constraints: 43

3.5.5 Generation-Demand Balance Constraints 43
3.5.6 Market Residual Supply and Demand Price-Quota Curves 44
3.5.7 Uncertain Critical Load and Renewable Generation: 44
3.5.8 Profit Function 45
3.6 Solution Methodology 45
3.6.1 MILP Counterpart of the Bidding Model 46
3.6.2 Dantzig-Wolfe Decomposition Method 49
3.7 Case Study 50
3.7.1 Test System Setups 50
3.7.2 Simulation Results 54
3.8 Conclusion 57
4 Conclusion and Future Work 59
4.1 Conclusions and Contributions 59
4.2 Future Work 60
4.2.1 Real-Time Market Bidding Model 60
4.2.2 Advanced Uncertainty Modeling Method 60
4.2.3 Other Collaborations Among NMGs 61
4.2.4 Fair Porfit Allocation Method 61
References 62

List of Figures

Figure 1.1 Trend in global renewable energy installed capacity [7] 2

Figure 1.2 Forecast of global distributed generation capacity [8] 2

Figure 1.3 A typical microgrid configuration 4

Figure 1.4 Volatility in AESO pool prices (January to September, 2019) [34] 6

Figure 2.1 Illustration of scenario tree 15

Figure 2.2 Duck Curve in CAISO [60] 18

Figure 2.3 Flowchart for quantitative sub-hourly wind power ramp behavior modeling 20

Figure 2.4 KDE results of analysis on sub-hourly wind power ramp behaviors 27

Figure 2.5 IEEE 39 Bus test system 28

Figure 2.6 Identified worst-case wind power output 29

Figure 2.7 System ramp reserves and wind power ramp ranges 30

Figure 3.1 Semi-decentralized coordination framework of the NMGs 38

Figure 3.2 Market residual supply/demand price-quota curves 40

Figure 3.3 Illustration of Dantzig-Wolfe decomposition method 49

Figure 3.4 Scenarios of market residual supply/demand curves for selected day 53

Figure 3.5 Scheduled price-quantity offers/bids for hour 1 to hour 12 with the corresponding market residual supply/demand curves 54

Figure 3.6 Scheduled price-quantity offers/bids for hour 13 to hour 24 with the corresponding market residual supply/demand curves 55

Figure 3.7 Comparison between price-taker and price-maker bidding strategy for the scheduled day 56

List of Tables

Table 3.1 Setups of individual microgrids 50

Table 3.2 Capacity limits on transmission lines between individual MGs 51

Table 3.3 Setups of uncertainty parameters 52

List of Abbreviations

BD	Benders Decomposition.
C&CG	Column and Constraint Generation.
DAUC	Day-Ahead Unit Commitment.
DDG	Dispatchable Distributed Generator.
DisCo	Distribution Company.
DL	Deferrable Load
DWD	Dantzig-Wolfe Decomposition.
ESS	Battery Energy Storage System.
GenCo	Generation Company.
GHG	Green House Gas.
KDE	Kernel Density Estimation.
MG	Microgrid.
MILP	Mixed Integer Linear Programming.
MINLP	Mixed Integer Non-Linear Programming.
NDG	Non-Dispatchable Distributed Generator.
NMG	Networked Microgrids.
PHEV	Plug-in Hybrid Electric Vehicle.
P2P	Peer-to-peer.
RES	Renewable Energy Sources.
RO	Robust Optimization.

SF	Shifting Factors.
SP	Stochastic Programming.
SOC	State of Charge

1 Introduction

1.1 Background

Over the last few years, changes in the consumers' needs have been driving the reshapes in the electric power industry. In general, these changes are fueled by the following three aspects: (a) economic requirements; (b) environmental requirements; (c) technical requirements. Economic needs mean that, with the increase in consumption, customers now are looking for more affordable electricity. Environmental needs mean customers are concerning about the environmental pollution and the fossil fuel depletion caused by conventional generators, alternatively they are looking for other cleaner energy sources. The technical needs mean that, during some most recent natural disasters, customers find that existing power systems cannot withstand these extreme conditions all the time, more reliable power supply sources are needed in case of emergency [1],[2].

Driving by the above three emerging requirements, evolutions in power systems are taking place on both the generation side and the demand side. In terms of the generation side, on the one hand, driven by the government environmental-friendly policies, world-widely more and more renewable generators are being installed over the last few years or planned to be installed in the near future, with the form such as solar, wind, hydro, tidal, etc [3]. As shown in Figure 1.1, the global total installed renewable generation has doubled by 2018 compared with 2009. On the other hand, more and more conventional generators that rely on fossil fuel are being retired [4]. As a result, renewable generation is continuously taking more shares. However, the environmental benefits of renewable generation do not come without cost. Clean energy can cause as many problems as it may solve. The intermittency of renewable generation brings a lot of challenges to the daily operation of power systems, such as more and more severe ramp events in net load profiles, mismatches between peak generation and peak demand, etc [5],[6].

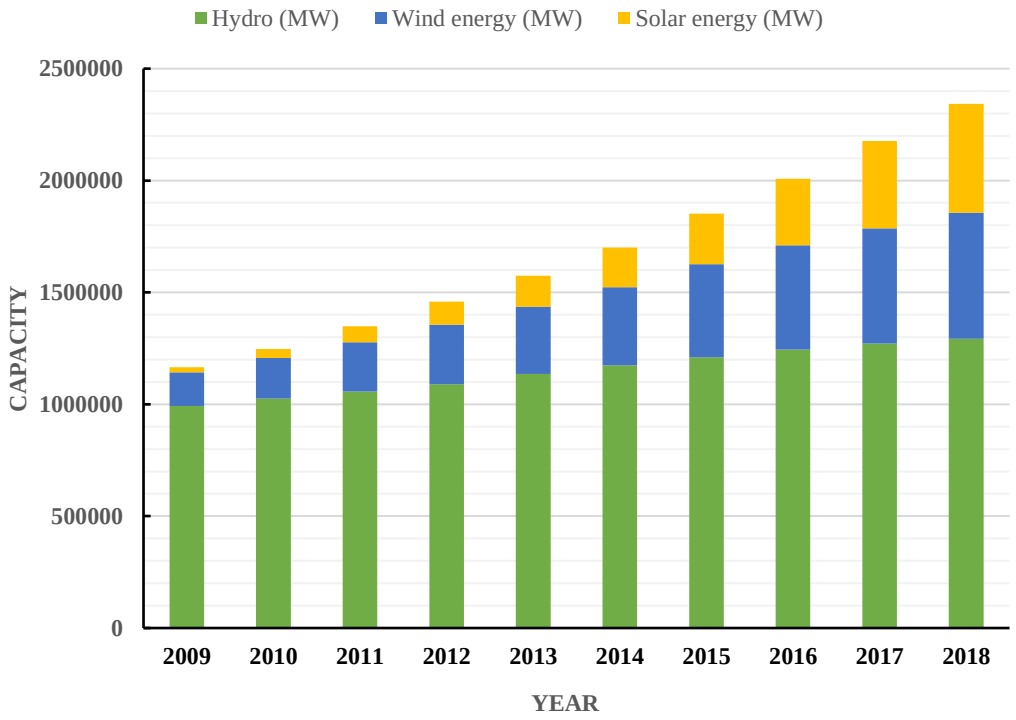

Figure 1.1 Trend in global renewable energy installed capacity [7]

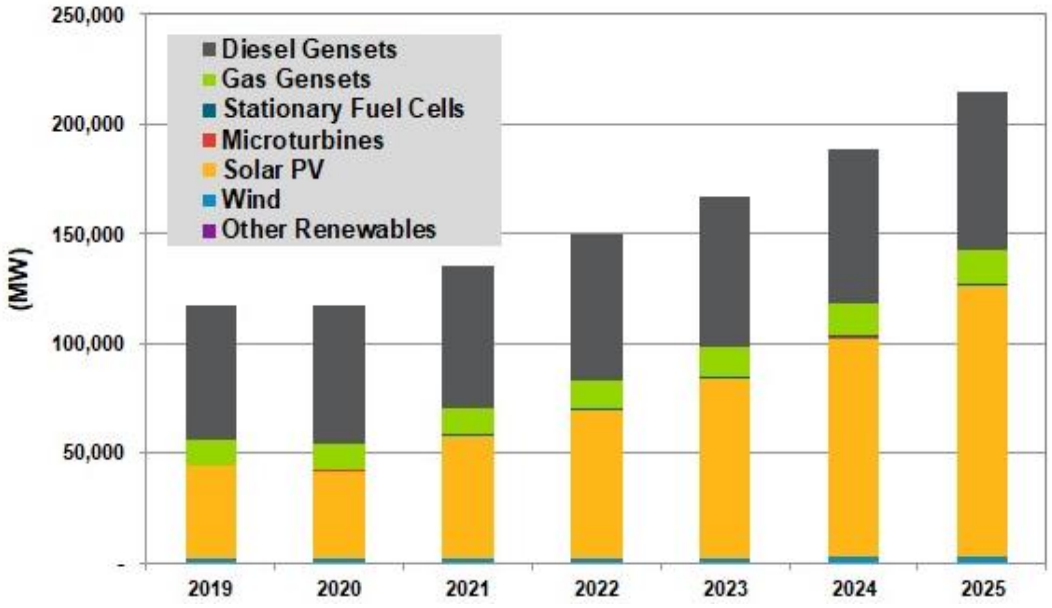

Figure 1.2 Forecast of global distributed generation capacity [8]

In terms of the demand side, consumers now are looking for a more reliable, affordable, and high-quality power supply. Interruptions in electricity supply are unbearable for many consumers,

especially for those sensitive consumers such as chips factory and big data centers [9]. Traditional centralized power systems are vulnerable to disasters, no matter natural ones (tsunami, hurricane, earthquake, and wild-fire) or man-made ones (cyber-attacks). It will take a long time to recover from a major outage [10]. As a result, nowadays more and more people are turning to distributed on-site generation for more reliable and resilience power supply. As shown in Figure 1.2, global deployment of distributed generation is expected to be doubled by 2025. However, these on-site energy resources also bring many problems to the daily operations of power systems, including increased short circuit levels, coordination between utility grid protection and DG protection measures, etc [11].

Microgrids have been regarded as promising solutions to solve the above problems and facilitate the transition into future power systems [13]. Microgrids are continuously gaining value in contemporary power systems and will continue to be valuable in future systems. Nowadays, microgrids can be found in hospitals, mining sites, factories, as well as university campuses. It is expected that annual revenue of microgrids will grow from $2.4 billion by 2016 to approximately $6 billion by 2023 [14]. According to the IEEE standard (IEEE Std. 2030.7) [15], a microgrid is defined as a group of distributed energy resources that are interconnected with each other inside a specific electric boundary. A microgrid can be connected to, or disconnected from the utility grid through the point of common coupling (PCC). By changing the connection status with the utility grid, a microgrid can operate in either grid-connected mode or islanded mode. A microgrid can be owned by either the system operator or a consumer. The key components of a microgrid may include, but not limited to the following energy sources: (a) dispatchable conventional generators, including combined heat and power units (CHP), fuel cells, diesel generators, micro-turbines; (b) non-dispatchable renewable generators, including solar, wind, small hydro, tidal generation; (c) energy storage systems; (d) responsive demands [16]. A typical microgrid configuration is demonstrated in Figure1.3.

1.2 Development of Microgrids

1.2.1 Configurations of Microgrids

Microgrids can be configured in different forms to serve different purposes [17]. With the development of microgrids, the configurations of microgrids will continue to change. Typical configurations may include: (a) authentic microgrids, which are self-governed and operated by the consumers, many of the currently deployed microgrids fit this category, including most demonstration projects like university campus microgrids; (b) virtual microgrids, which coordinates multiple DERs, such as EVs and DGs that located on different sites, to interact with the utility grid as a single dispatchable entity; (c) remote microgrids, which are operated in off-grid mode to serve the electricity needs of remote off-grid communities, mining sites and military bases. [18]. Generally, a microgrid is configured as shown in Figure 1.3.

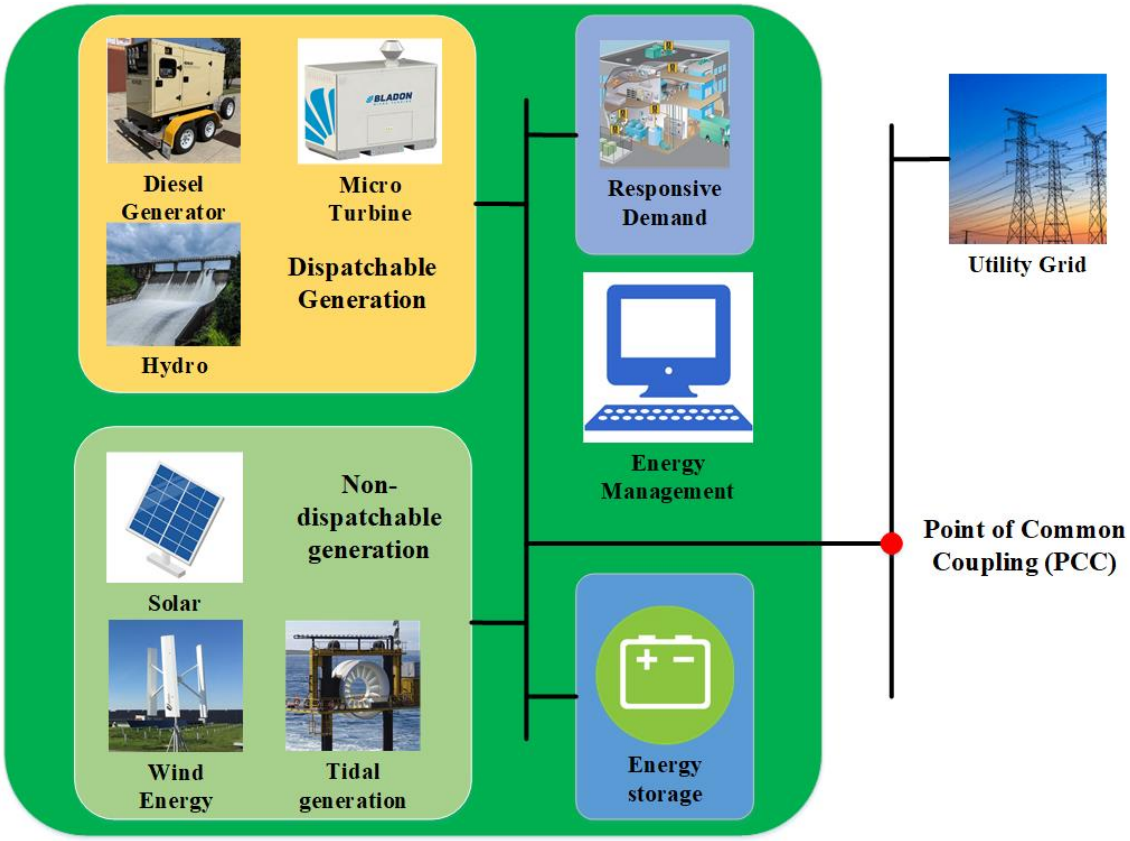

Figure 1.3 A typical microgrid configuration

1.2.2 Benefits of Microgrids

In conclusion, microgrids have the following benefits:

- Microgrids can enhance the utility grid's overall security and resiliency by providing necessary supports to the utility grid during catastrophic events. [10], [19]. Microgrids have proved themselves to be partners of utility grids during several major outages. For example, during the wildfire in 2007 in California State, the microgrid of University of California (San Diego) quickly responded and provided power support the system [22]. Another example is the campus microgrid located at New York University. In 2012, when Hurricane Sandy hit New York City and cut power to most parts of the downtown area, thanks to the microgrid, New York University was able to keep electricity supply [23].

- Microgrids can help those consumers who have high expectations in power quality and reliability [24]. Microgrids can reduce the consumers' dependence on the utility grid and alternatively guarantee a more reliable, comprehensive, and environmental-friendly power supply to sensitive consumers, such as hospitals, factories, and military bases. On the one hand, microgrids provide near-demand generation, which can avoid most of the transmission and distribution power losses [19]. On the other hand, microgrids provide higher energy utilization rates of distributed energy sources, especially for renewable generation and energy storage devices. Due to the parallel and flexible operation mode, microgrids enable locally-customized operation schedules for DERs [20], [21].

- Microgrids can facilitate economic development. For one thing, deployments of microgrids will create more jobs, especially at local levels. Contractors, electricians, engineers, and researchers are needed in the planning, construction, and daily maintenance [25]. For another thing, energy transactions with the utility grid can increase the revenue of microgrid owners. This will further in return promote the investment into microgrid projects.

1.2.3 Current Studies on Microgrids

Microgrid has been a very popular research topic in recent years. There have been extensive studies focusing on different aspects of microgrids, including both technical ones and economic ones. In terms of economic studies on microgrids, in recent years the energy transactions problems between microgrids and the utility grid have been a hot topic. With the capability of bi-directional energy transfer with the utility grid, fully-developed microgrids generally play as prosumers in the context of electricity market because they can either sell excessive energy generated by DERs to the utility grid when there is shortage in electricity supply, or purchase electricity from the utility grid when there is surplus in electricity supply. In addition to energy services, microgrids are also able to provide ancillary services to the utility grid, including the frequency regulation, reactive power and voltage control, spinning or non-spinning services, and the recently emerging flexible ramp products. [26][27][28].

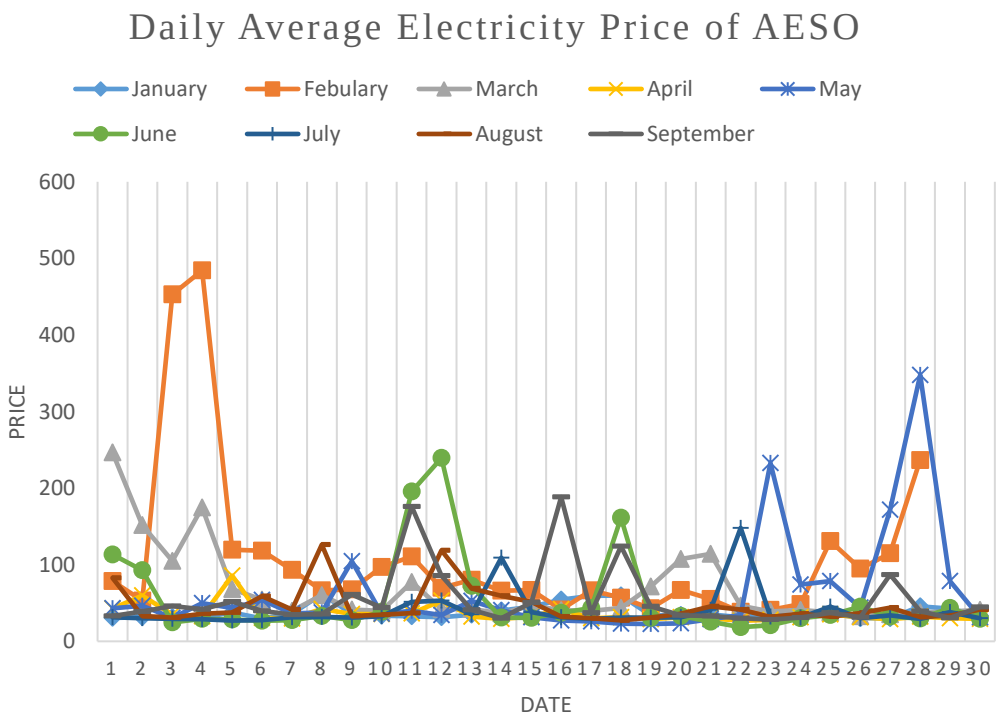

Figure 1.4 Volatility in AESO pool prices (January to September, 2019) [34]

This thesis focuses on developing optimal bidding strategies for microgrids in providing energy services. As shown in Figure 1.4, the volatility in market prices provides sufficient arbitrage

opportunities to microgrids. To achieve full benefits of microgrids and maximize microgrids' revenue in the market, a proper bidding strategy is of fundamental importance. This bidding model should be able to properly model the operations of individual DERs and mitigate uncertainties in the model. There have been extensive studies on the optimal energy management and bidding problems of microgrids. Microgrids are generally taken as price-takers in the market due to their relatively small capacity [29]. An optimal bidding strategy for microgrids in the day-ahead joint energy and ancillary service market is proposed in [26]. A three-stage robust-stochastic hybrid optimization based optimal bidding strategy considering flexible demands is proposed in [29]. A two-stage stochastic optimal bidding strategy considering consumers' electricity and thermal needs is proposed in [30].

Considering that in the future there will be many microgrids in the system, MGs' participation in the market presents a new problem. Most recent studies now begin focusing on the coordination problems between individual MGs when participating in the electricity market. Relations between individual MGs in the market can be summarized into two types: (a) non-collaborative; and (b) collaborative relations. Generally, the former non-collaborative relations involve the peer-to-peer (P2P) energy transactions between individual microgrids. This P2P transaction process can be modeled using non-cooperative game theories. [31][32]. However, there exists doubt about the real-world application feasibility of such P2P energy transactions. While in terms of the collaboration between MGs, individual MGs are networked and coordinated as a single dispatchable entity to participate in the market. This microgrids aggregation is further referred as networked microgrids (NMGs). The NMGs can avoid the problems caused by interconnections between each MG and the utility grids. What's more, bidding models for a microgrid generally assume the MG to be price-takers due to their limited capacity, while the cooperative coordination between individual microgrids enables the NMGs entity to have a large aggregated capacity to compete with others in the market, and finally have impacts on the market price. [33]

1.3 Problems Statement

1.3.1 Price-Maker Bidding Strategy

As mentioned above, the cooperatively coordinated networked microgrids cluster will have an aggregated capacity that is big enough to have influence on the market prices. This NMGs entity is able to submit either supply offers or demand bids to the market. In other words the NMGs entity plays as competitors of distribution companies (DisCos) or generation companies (GenCos). In this case, a price-maker bidding strategy that considers the operation models of individual DERs inside the NMGs entity is needed to maximize the NMGs' total net revenue from the market.

1.3.2 Optimization Method

There are multiple uncertainty sources in the optimization model, including the renewable generation, the demand, and the day-ahead market. If these uncertainties are not accommodated properly in the model, the obtained optimal decisions may be infeasible in real-world applications. As a result, proper methods are needed to deal with these uncertainties. In addition, the uncertainties should be modeled in a computationally tractable way.

1.3.3 Coordination Framework for Microgrids

Individual microgrids in the NMG are coordinated to deliver the submitted bids to the market, which is the aggregated capacity of each microgrid. However, given the fact that each microgrid may belong to different stake-holders, the privacy concern of each microgrid must be addressed in the bidding model. Particularly, the solution method to the optimization model should obtain the optimal operation schedule while given maximum level protection to the privacy of each microgrid.

1.4 Research Objectives

Based on the research problems discussed in previous sections, this thesis aims at developing the optimal coordination framework of a networked microgrids cluster. Under this framework, multiple interconnected microgrids are coordinated as a single dispatchable entity that is able to

participate in the pool-based electricity market. In particular, three objectives are dealt with sequentially in this thesis as follow:

- Identify and discuss the uncertainty sources in the bidding model;
- Propose an optimization framework for offering or bidding strategies under uncertainty;
- Solve the optimization problem with a privacy-preserved algorithm.

1.5 Thesis Outline

This thesis is organized in a manuscript style. To be specific, two main chapters of this thesis are based on two manuscripts respectively. Details of the modeling approach have been covered in these two chapters. Individual chapters are closely related to each other so that the research objective of this thesis is obtained sequentially.

Chapter 1 puts forward the background and motivations behind this research. The concept, development, and current studies on microgrids are briefly reviewed. The challenges, opportunities, and benefits of microgrids in future power systems are also discussed in this chapter. This chapter also describes the research problems that are addressed in this thesis. The research objectives of this thesis are summarized in this chapter.

Chapter 2 focuses on optimization methods under uncertainties. Common optimization methods in recent years are briefly reviewed and discussed in this chapter. An improved day-ahead unit commitment model that considers the sub-hourly wind power ramp behaviors is presented to illustrate the implementation and solution method to a 2-stage adaptive robust optimization model. The work presented in this chapter is based on the paper: Flexible Robust Unit Commitment Considering Sub-hourly Wind Power Ramp Behaviors..

Chapter 3 presents an optimal price-maker bidding strategy for networked microgrids that aims at maximizing the total net revenue from electricity trading in the day-ahead market. In terms of microgrids' owners, this bidding strategy can maximize the total net revenue of microgrid owners, and provide the system operators with more flexibility to accommodate the electricity shortage caused by severe ramping events in net load profile. The paper: A Price-Maker Bidding Model for Networked Microgrids in Day-Ahead Electricity Market forms the basis of the work presented in this chapter.

Chapter 4 summarizes the work in this thesis. Key findings are highlighted in this chapter. Further, suggestions for future research directions are presented as well.

2 Optimization under Uncertainty

2.1 Abstract

In this chapter, Common uncertainty management methods in optimization problems are review and compared. A robust DAUC model that specifically considers the sub-hourly ramping behaviors of wind generation is presented here to illustrate the implementation of uncertainty management in optimization problems. The DAUC model is chosen here for the following two reasons: (a) In terms of system-level optimization, there are a lot of similarities between microgrids models and UC models; (b) There have been extensive methods for modeling UC under uncertainties, where these methods can serve as references for the modeling of NMGs under uncertainties.

2.2 Nomenclature

Set/indices

t/T	Indices/sets for scheduling time horizon.
$g/\mathcal{G}_{\mathrm{b}}$	Indices/sets for generators at bus b.
b/B	Indices/sets for considered buses.
r/R	Indices/sets for wind power generators.
$i \in \mathrm{Seg}_{\mathrm{g}}^{\mathrm{b}}$	Segments of piecewise linear generation cost functions.
l/L	Indices/sets for transmission lines.

Parameters

UT_g^b	Minimum up-time of generator g.
DT_g^b	Minimum down-time of generator g.

$\overline{\mathrm{PC}_g^b}$ Maximum output of generator g.

$\underline{\mathrm{PC}_g^b}$ Minimum output of generator g.

CRU_g^b Maximum ramp up capacity of generator g.

CRD_g^b Maximum ramp down capacity of generator g.

$\mathrm{C}_g^{b,min}$ Coefficients related to the piecewise linear generation cost function.

Slp_{gi}^b Slope of each segment of the piecewise linear generation cost function.

$\mathrm{F}_l^{\max}$ Maximum transmission capacity of line l.

SF_{lb} Shifting factor of the transmission line l.

RUR_a Coefficients of functions that estimate the ramp-up capacity requirements.

RUR_b Coefficients of functions that estimate the ramp-up capacity requirements.

RDR_a Coefficients of functions that estimate the ramp down capacity requirements.

RDR_b Coefficients of functions that estimate the ramp down capacity requirements.

D_t^b Total demand at bus b in time slot t.

$\overline{\mathrm{WP}_{rt}^n}$ Central forecast value of wind generator r.

$\mathrm{WP}_{rt}^{\mathrm{U}}$ Upper bound of the wind power output.

$\mathrm{WP}_{rt}^{\mathrm{L}}$ Lower bound of the wind power output.

Decision variables

su_{gt}^b The start-up flag of generator g on bus b at the beginning of time t.

sd_{gt}^b The shut-down flag of generator g on bus b at the beginning of time t.

f_{gt}^b The operation cost of generator g on bus b during time slot t.

x_{gt}^b On/off status of generator g.

p_{gt}^{b} Power reference of generator g.

$\mathcal{R}u_t$ System sub-hourly ramp up capacity requirements.

$\mathcal{R}d_t$ System sub-hourly ramp down capacity requirements.

wp_{rt} Uncertain output of wind generation r.

2.3 Introduction

With the rapid changes in power system, more and more uncertainty sources are introduced into the power system operation, this conclusion holds in all aspects from generation (renewable energy integration), transmission (dynamic thermal rating), distribution and consumption (responsive demands). Uncertainties can make huge difference in power system models, if not dealt with properly, uncertainties will make the so-called optimal solution become infeasible in real-world applications. As a result, the uncertainties managements are becoming more and more important in optimization problems for power system operation and planning, including unit commitment problem (UC), economical dispatch (ED), transmission system expansion, etc. How to model and represent impacts of uncertainties appropriately in optimization models has drowned many attentions from both industries and academics. It is generally required that the uncertainty formulations should be both accurate and computationally tractable. In this thesis, to conclude the development of optimization under uncertainty in power system operations, the UC problems are taken as examples. In recent years, there have been extensive studies on solving UC problems under uncertainty. In terms of uncertainty formulations in the UC models, the most general approaches can be summarized into two categories that are respectively stochastic optimization (SO) approaches and the robust optimization (RO) approaches.

2.3.1 Stochastic Optimization Methods

In the SO frameworks, uncertain parameters are represented by scenarios, which are generated (usually by Monte Carlo method) from the corresponding estimated probability density function (PDF). The PDFs are usually derived from historical data. Each scenario is regarded as a typical realization of the uncertain parameters and is assigned with a probability. According to the stages

of decision making process in the model, there are generally two types of stochastic optimization frameworks, one is the 2-stage SO, and the other one is the multi-stage SO. In terms of the 2-stage SO, in the first stage the typical scenarios with their corresponding probability are generated from the PDFs, then in the second stage the decisions are made to minimize the total expected operational cost. The 2-stage SOUC problems are presented in the following compact forms [35]–[39]:

$$\min_{\mathbf{u}\in\mathcal{U}} \mathbf{b}^{\mathbf{T}}\boldsymbol{x} + \mathrm{Exp}[f(\boldsymbol{u},\boldsymbol{y})] \tag{2.1}$$

s.t.

$$\mathrm{Exp}[f(\boldsymbol{u},\boldsymbol{y})] = \sum p_u min \mathbf{c}^{\mathbf{T}} y \tag{2.2}$$

$$\mathrm{Au} + \mathrm{B}y + \mathrm{C}x \leq \mathrm{d} \tag{2.3}$$

Where the u represents the uncertain parameters, x represents the day-ahead decision variables (the on/off status of individual generators), y represents the real-time decision variables (power reference and reserve margin of individual generators). The objective function of the 2-stage stochastic programming is to minimize the total expected operation cost.

While for the multi-stage SOUC models, the objective function also aims at minimizing the total expected operation cost. However, in contrast to the 2-stage ones which only consider the uncertainties one time, the uncertainties in multi-stage stochastic optimization models are revealed dynamically and gradually over the whole scheduling time horizon [40]–[42]. To facilitate such uncertainty modeling method, scenario trees are used which is illustrated in Figure 2.1.

A scenario tree is a reduced form that stimulates the reveal process of uncertainty scenarios. This tree clusters those uncertainty realizations into a set of branches with specified probabilities of occurrence. The tree comprises of S scenarios, with each scenario contains t nodes that equals to the time slot numbers. Starting from the root node (initial time slot t_0), the tree continues to branch out through the following time slots. When $t = \mathrm{T}$, the tree terminates, with each node solely belongs to one scenario. Each scenario equals one unique path starting from the root node to the leaf node. A probability p_i is assigned to each scenario i, the sum of p_i is 1.

In this multi-stage framework, based on the revealed uncertainties of previous time slots, the PDFs of later time slots are updated sequentially. To release the computational burden of this

method, scenario reduction methods are also needed. As shown in the above figure, one scenario is equivalent to a unique path starting from the root node (the starting time slot) to the leaf node (the end time slot).

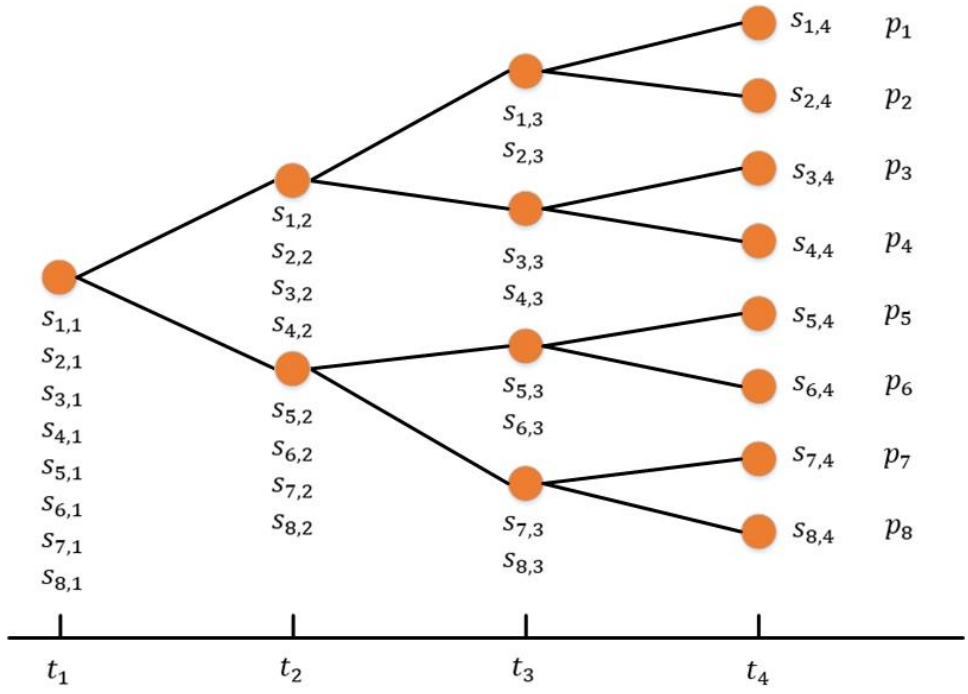

Figure 2.1 Illustration of a scenario tree

2.3.2 Robust Optimization Methods

Different from SO frameworks, which rely on the PDF of the uncertain parameters, the robust optimization (RO) frameworks rely on the discrete finite deterministic uncertainty sets to model uncertain parameters. Similar to SO approaches, the RO frameworks can also be summarized into two categories based on the stages of uncertainty representation, one is the 2-stage RO, and the other one is the multi-stage RO. The formulations of the 2-stage RO framework has the following compact form:

$$\min_{\boldsymbol{u}\in\mathcal{U}} \mathbf{b}^{\mathbf{T}}\boldsymbol{x} + \max f(\boldsymbol{u},\boldsymbol{y}) \tag{2.4}$$

s.t.

$$f(\boldsymbol{u},\boldsymbol{y}) = \min \mathbf{c}^{\mathbf{T}} y \tag{2.5}$$

$$\mathbf{A}\boldsymbol{u} + \mathbf{B}\boldsymbol{y} + \mathbf{C}\boldsymbol{x} \leq \mathbf{d} \tag{2.6}$$

Where A is the coefficient matrix corresponding to the constraints related to uncertain parameters u, B is the coefficient matrix corresponding to the constraints related to second stage decision variables y, C is the coefficient matrix corresponding to the first stage decision variables x. d is the vector of right hand constraints.

In the 2-stage robust optimization framework, the uncertain parameters $\boldsymbol{u}$ are modeled using a deterministic uncertainty set $\mathcal{U}$. Details of defining this uncertainty set are covered in the following sections. The objective of the 2-stage robust model is to guarantee that the decisions are feasible in terms of any realizations of the uncertain parameters modeled by the uncertainty set, and at the same time the total operation cost corresponding to the worst-case realizations of uncertain parameters is minimized. In this two-stage framework, the on/off decisions are made in the first stage, while the economic dispatch decisions are made in the second stage [43]–[45]

Comparing with SOUC models, ROUC models are generally more computationally efficient. However, there is one major problem with these 2-stage models. The second stage decision variables are made under an important assumption that the uncertainty parameters over the whole scheduling horizon have been fully revealed. While in real-world applications, the decisions in power system operations are made sequentially, which means the decisions should be made only based on the information that is realized up to that hour. The assumptions of the 2-stage model may violate the *nonparticipativity* rule. To resolve this issue of 2-stage models, in recent studies, a multi-stage robust optimization framework is developed, where the uncertainty sets of future time slots are dynamically adjusted as the uncertain parameters of previous time slots revealed. However, this framework also introduces higher computational burden. To solve the accompanying challenges, linear affine policies are widely employed. The formulations of multistage RO have the following compact form [46]–[48]:

$$\min_{\boldsymbol{u}\in\mathcal{U}} \mathbf{b}^{\mathbf{T}}\boldsymbol{x} + \max f(\boldsymbol{u},\boldsymbol{y}) \tag{2.7}$$

s.t.

$$f(\boldsymbol{u},\boldsymbol{y}) = \min \sum_{t=1}^{T} \mathbf{c}^{\mathbf{T}} y_t \tag{2.8}$$

$$\mathbf{A}\boldsymbol{u} + \mathbf{C}\boldsymbol{x} \leq \mathbf{d} \tag{2.9}$$

$$\boldsymbol{y}_t = \boldsymbol{g}(\boldsymbol{u}_1 \dots \boldsymbol{u}_{t-1}) \tag{2.10}$$

2.3.3 Other Methods

Both RO methods and SO methods have their respective advantages. Robust optimization methods do not rely on exact PDFs of uncertain parameters, which is the most silent distinction between this method and the SO ones. However, if the PDFs of uncertain parameters are available, the results of RO methods will be over-conservative. To bridge the gap between the conservativeness of RO approaches and the specificity of SO approaches, a more sophisticated optimization framework has been proposed and is becoming more and more popular in recent years. This method is called distributionally robust optimization (DRO). [49][50]. DRO can be viewed as a hybrid of the above-mentioned robust optimization and stochastic optimization methods. The uncertain parameters are modeled using an ambiguity set, which is a family set of all possible PDFs of the uncertain parameters. It is assumed that the actual PDF of the uncertainties is contained in this set. Comparing with conventional RO models, DRO is able to interpret the uncertain parameters more appropriately as it can capture the underlying distribution information. While comparing with SO methods, DRO is more practical as specific information on the joint PDF of uncertain parameters is not needed to construct ambiguity set. The objective function of the DRO aims at maximizing the. The DRO methods have been employed to solve a broad variety of problems in the area of power system, including energy and reserve schedule problems, renewable generation planning, etc. As the core of the DRO models, the construction of ambiguity sets is also a popular topic in recent studies [51]–[56].

Apart from the method mentioned above, chance-constrained optimization (CCO) is also one of the major methods to solve optimization problems under uncertainties. In this method, the optimization problem is formulated that the probabilities of satisfying certain constraints are above a given level. In other words, the feasible region of the optimization problem is restricted to increase the confidential level of the solutions. However, the robustness of this method also brings in the difficulty in solving the model [57]–[59].

2.4 Flexible Robust DAUC Model

With the ever-increasing penetration level of wind power generation, management of the uncertainty and variability of wind power in day-ahead unit commitment (DAUC) problems have

received much attention in recent years. The focus of existing studies on DAUC considering uncertain wind power has mainly been on the hourly operation constraints. However, if the sub-hourly wind power variations are not carefully considered, the obtained unit commitment (UC) solutions may not be flexible enough to accommodate the sub-hourly wind variations and results in undesired wind curtailments. Lack of flexibility can lead to serious challenges for system daily operations. The infamous "Duck Curve", which is the net load profile of CAISO can be set as an example here. It can be observed in Figure 2.2 that, high renewable penetration level requires greater system flexibility, as more severe ramp events will occur in the net load profile.

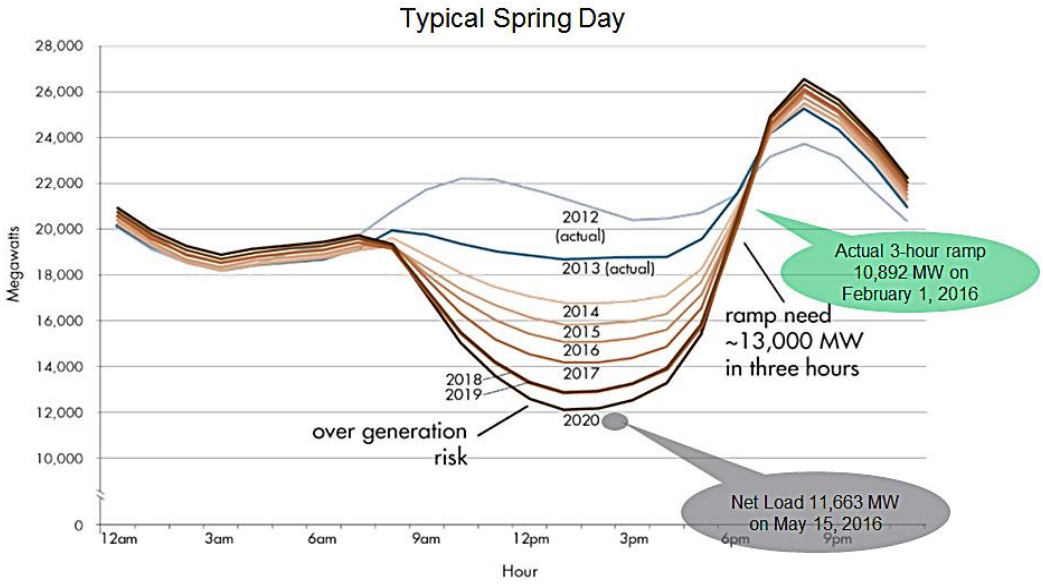

Figure 2.2 Duck Curve in CAISO [60].

To manage uncertainties of wind power and ensure the full utilization of it, in this chapter a robust optimization-based UC model considering sub-hourly wind power variation is proposed. The objective of this model is to provide a flexible and as well robust UC solution for the conventional thermal units, which guarantees sufficient ramp up and ramp down capacity reserves for the variations of wind power in the intra-hour time frame. Firstly, a non-parametric approach based on the 2-dimensional kernel density estimation is proposed to quantify the sub-hourly wind power variability. Then, based on the quantification results, a set of ramp constraints are imposed on the robust UC model. A column and constraint generation (C&CG) method is applied to solve the improved UC model. The proposed model is tested and compared with conventional UC models on IEEE 39 bus test system to verify its effectiveness.

2.5 Background

The reduction of greenhouse gas (GHG) has been a worldwide joint task in recent years. As a consequence, wind power penetration in the electricity generation side is intensively growing throughout the world. Integrations of wind power have sophisticated effects on power system operations. In practice, it is the system operator's duty to schedule the production of different kinds of power generations so that the real-time balance between supply and demand can be achieved. Such that wind power will generally be fully dispatched to their maximum allowable output before the conventional power generations are considered. However, the inherent uncertainty and variability of wind power make the system balancing more challenging [61]. The uncertainty refers to the fact that the output of wind power cannot be forecasted precisely in advance, and the variability refers to the fact that the wind power output can change volatilely in a very short time. These two characteristics greatly affect the operation schedules of conventional power plants, such as unit commitment (UC) and economic dispatch.

As an important power system planning tool, the day ahead unit commitment (DAUC) is presented to schedule the on/off status and approximate output for a set of generators, which subject to the corresponding device and system constraints, in an economical and reliable way to meet the forecasted demand [62]. In the context of increasing wind power penetration, the DAUC must be improved to accommodate the uncertainty and variability of wind power. There have been some studies on representing the uncertainty and variability of wind power in the DAUC model, but the focus has mainly been on the hourly operation because DAUC generally deals with hourly time steps. However, according to some analysis on the ramp behaviors of wind power [54],[55], it can sometimes exhibit non-monotonic behaviors and be more severe than the hourly average ramp rate. It means that with high penetration of wind power, the obtained UC solution satisfying the hourly operation requirements may not be feasible in the sub-hourly time horizon. Because the conventional generators may lack the ability to follow the rapid variations due to their technical operational constraints.

Motivated by the problems mentioned above, this chapter proposes a robust optimization (RO) based DAUC model that takes into account the hourly as well as the sub-hourly wind power variations. In this chapter firstly a non-parametric approach is proposed to quantify the correlation

between sub-hourly and hourly wind power variations, in this way the sub-hourly operation constraints can be incorporated into the hourly operation constrains. The RO approach is applied in this chapter to deal with the hourly wind power uncertainty. The DAUC problem is formulated as a 2-stage min-max problem to satisfy the sub-hourly operation constraints in an economic way. A C&CG decomposition algorithm is applied to obtain a robust UC solution

2.6 Model Formulation

2.6.1 Analysis of the Sub-hourly Wind Power Ramp Behaviors

To consider sub-hourly ramp behaviors of wind power output, it is necessary to firstly develop a systematic way to categorize these variations. Recently there have been some studies on analyzing statistical characteristics of wind power variations on different time scales [56],[57].

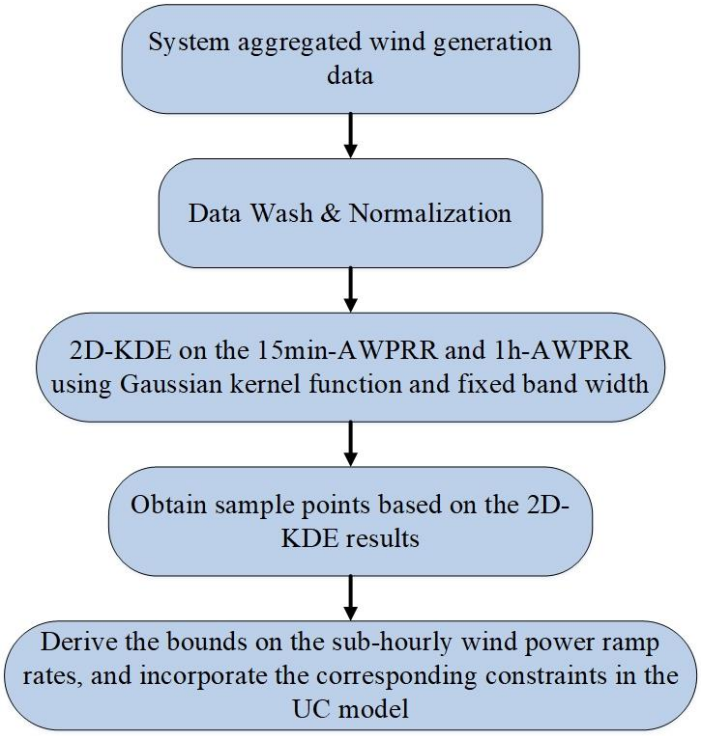

Figure 2.3 Flowchart for quantitative sub-hourly wind power ramp behavior modeling

However, the correlations between wind power variations on different time scales are neglected. As the DAUC decisions are made on hourly-basis, quantification of the correlation between sub-hourly ramp rate and average hourly ramp rate can facilitate incorporating the sub-hourly ramp constraints into hourly constraints in the DAUC model. As pointed in [67], the non-parametric

approach can represent the wind power variation characteristics more accurately. Thus, in this chapter, a 2-dimension kernel density estimation (2D-KDE) based approach is proposed. To be specific, in the following analysis we used the complete 2017 year aggregated 15-minute average wind power ramp rate (15min-AWPRR) and the 1-hour average wind power ramp rate (1h-AWPRR) data from Belgian TSO ELIA's data archive [68]. Such sampling frequency is appropriate for our study.

The 2D-KDE is calculated using the following equation:

$$\hat{f}(\boldsymbol{x}, \mathbf{H}) = \frac{1}{n}\sum_{i=1}^{n} K_{\mathbf{H}}(x - x_i) \tag{2.11}$$

Where the two data sets 15min-AWPRR $x_{1i} = [x_{11,}x_{12}, x_{13}, \dots x_{1n}]$ and 1h-AWPRR $x_{2i} = [x_{21,}x_{22}, x_{23}, \dots x_{2n}]$ are represented using $x_i = (x_{1i}, x_{2i})$. **H** represents the bandwidth matrix. Then based on the 2D-KDE results, quantile regression method is applied to derive the upper and lower bound of the sub-hourly wind power ramp ranges. The full data analysis procedure in the proposed method for the sub-hourly wind power ramp behaviors are concluded as Figure 2.3.

2.6.2 Improved 2-Stage Robust DAUC Model Considering Sub-Hourly Wind Power Ramp Behaviors

After analyzing the sub-hourly ramp behaviors of wind power variations, a 2-stage adaptive robust DAUC model incorporating the discovered sub-hourly ramp behaviors is developed here. The uncertain wind power is modeled with an uncertainty set. It is assumed that the uncertain wind power is within an interval $[\widehat{\mathrm{WP}}_{rt}^{\mathrm{L}},\ \widehat{\mathrm{WP}}_{rt}^{\mathrm{U}}]$ with the central forecast value to be $\overline{\mathrm{WP}}_{rt}^{\mathrm{F}}$ [69], where r/R is the index/set for wind turbines. This interval can be defined by quantiles using historical data or wind power forecast data. For instance, we can set $\widehat{\mathrm{WP}}_{rt}^{\mathrm{U}}$ and $\widehat{\mathrm{WP}}_{rt}^{\mathrm{L}}$ equal to the 0.95 and 0.05 quantiles of the random wind power output, respectively. In addition, an integer Γ_b called uncertainty budget is introduced to control the conservativism of the proposed model. This integer is regarded as the robust coefficient to control the system conservativism. Based on the bounds derived in [70], the robust coefficient is set as $\Gamma_b \geq 1.64\sqrt{24} = 8$ in this chapter. Correspondingly, the uncertainty set can be described as:

$$\mathcal{U} \coloneqq \Bigg\{ \mathbb{R}^{|\mathrm{B}|\times \mathrm{T}} : wp_{rt} = \overline{\mathrm{WP}}_{rt}^{\mathrm{F}} + z_{rt}^{+}\mathrm{WP}_{rt}^{\mathrm{U}} + z_{rt}^{-}\mathrm{WP}_{rt}^{\mathrm{L}}, \sum_{t=1}^{T}(z_{rt}^{+} + z_{rt}^{-}) \le \Gamma_b, \forall b \in \mathrm{B}, \forall r \in \mathrm{R}, \forall t \in \mathrm{T} \Bigg\} \tag{2.12}$$

where, $\overline{\mathrm{WP}}_{rt}^{\mathrm{F}}$ is the forecasted mean value, z_{rt}^{+} and z_{rt}^{-} are binary variables that indicate the wind power reaches the upper bound or the lower bound, $\mathrm{WP}_{rt}^{\mathrm{U}}$ and $\mathrm{WP}_{rt}^{\mathrm{L}}$ are the deviations from upper and lower bounds, respectively.

Based on the uncertainty set description and the quantified sub-hourly wind power ramp behaviors, the 2-stage robust optimization formulations are proposed to address the sub-hourly wind power variations.

$$\min_{x,su,sd} \sum_{t=1}^{\mathrm{T}}\sum_{b=1}^{\mathrm{B}}\sum_{g=1}^{\mathrm{G_b}}\left(su_{gt}^{b} + sd_{gt}^{b}\right) + \max_{wp\in\mathcal{U}} \min_{y\in\mathcal{X}(y)} \sum_{t=1}^{\mathrm{T}}\sum_{b=1}^{\mathrm{B}}\sum_{g=1}^{\mathrm{G_b}} f_{gt}^{b} \tag{2.13}$$

s.t.

$$\sum_{k=1}^{\mathrm{G}_g^b}(1 - x_{gk}^{b}), \forall k = \mathrm{G}_g^b + 1, \cdots, \mathrm{T} - \mathrm{UT}_g^b + 1 \tag{2.14}$$

$$\sum_{n=k}^{\mathrm{T}}\left[x_{gn}^{b} - \left(x_{gk}^{b} - x_{g(k-1)}^{b}\right)\right] \ge 0, \forall k = \mathrm{T} - \mathrm{UT}_g^b + 2, \cdots, T \tag{2.15}$$

$$\sum_{k=1}^{L_g^b} x_{gk}^{b} = 0 \tag{2.16}$$

$$\sum_{n=k}^{k+DT_g^b-1}\left(1 - x_{gn}^{b}\right) \ge \mathrm{DT}_g^b\left(x_{g(k-1)}^{b} - x_{gk}^{b}\right), \forall k = L_g^b + 1, \cdots, \mathrm{T} - DT_g^b + 1 \tag{2.17}$$

$$\sum_{n=k}^{T}\left[1 - x_{gn}^{b} - \left(x_{g(k-1)}^{b} - x_{gk}^{b}\right)\right] \ge 0, \forall k = T - \mathrm{DT}_g^b + 2, \cdots, T \tag{2.18}$$

$$su_{gt}^{b} \ge \left(x_{gt}^{b} - x_{g(t-1)}^{b}\right)SU_g^b \tag{2.19}$$

$$sd_{gt}^{b} \geq \left(x_{g(t-1)}^{b} - x_{gt}^{b}\right) SD_{g}^{b} \tag{2.20}$$

$$\forall t \in \mathrm{T}, \forall b \in \mathrm{B}, \forall g \in \mathrm{G}_{b}$$

Where,

$$\mathcal{X}(y) := \sum_{b=1}^{\mathrm{B}} \left(\sum_{g=1}^{\mathrm{G}_{b}} p_{gt}^{b} + \sum_{r=1}^{\mathrm{R}} wp_{rt} \right) = \sum_{b=1}^{\mathrm{B}} \mathrm{D}_{t}^{b} \tag{2.21}$$

$$\left| \sum_{b=1}^{\mathrm{B}} \left[\mathrm{SF}_{lb} \left(\sum_{g=1}^{\mathrm{G}_{b}} p_{gt}^{b} + \sum_{r=1}^{\mathcal{R}} wp_{rt} - \mathrm{D}_{t}^{b} \right) \right] \right| \leq \mathrm{F}_{l}^{\max} \tag{2.22}$$

$$f_{gt}^{b} \geq \mathrm{C}_{g}^{b,min} x_{gt}^{b} + \sum_{i=1}^{\mathrm{Seg}_{g}^{b}} \mathrm{Slp}_{gi}^{b} \, \delta_{gt,i}^{b} \tag{2.23}$$

$$\underline{\mathrm{PC}}_{g}^{b} x_{gt}^{b} \leq p_{gt}^{b} \leq \overline{\mathrm{PC}}_{g}^{b} x_{gt}^{b} \tag{2.24}$$

$$p_{gt}^{b} - p_{g(t-1)}^{b} \leq \left(2 - x_{g(t-1)}^{b} - x_{gt}^{b}\right) \underline{\mathrm{PC}}_{g}^{b} + \left(1 + x_{g(t-1)}^{b} - x_{gt}^{b}\right) \mathrm{CRU}_{g}^{b} \tag{2.25}$$

$$p_{gt}^{b} - p_{g(t-1)}^{b} \leq \left(2 - x_{g(t-1)}^{b} - x_{gt}^{b}\right) \underline{\mathrm{PC}}_{g}^{b} + \left(1 - x_{g(t-1)}^{b} + x_{gt}^{b}\right) \mathrm{CRD}_{g}^{b} \tag{2.26}$$

$$0 \leq \mathrm{ru}_{gt}^{b} \leq CRU_{g}^{b} \tag{2.27}$$

$$ru_{gt}^{b} \leq [(\overline{\mathrm{PC}}_{g}^{b} - p_{gt}^{b}) x_{gt}^{b}]/1\mathrm{h} \tag{2.28}$$

$$\sum_{b=1}^{\mathrm{B}} \sum_{g=1}^{\mathrm{G}_{b}} ru_{gt}^{b} \geq \mathcal{R}u_{t} \tag{2.29}$$

$$0 \leq rd_{gt}^{b} \leq \mathrm{CRD}_{g}^{b} \tag{2.30}$$

$$rd_{gt}^{b} \leq [\left(p_{gt}^{b} - \underline{\mathrm{PC}}_{g}^{b}\right) x_{gt}^{b}]/1\mathrm{h} \tag{2.31}$$

$$\sum_{b=1}^{\mathrm{B}}\sum_{g=1}^{\mathrm{G}_b} rd_{gt}^{b} \geq \mathcal{R}d_t \tag{2.32}$$

$$\mathcal{R}u_t = \max\{\mathrm{RUR}_a \times \left(wp_{rt} - wp_{r(t-1)}\right)/60 + \mathrm{RUR}_b, 0\} \tag{2.33}$$

$$\mathcal{R}d_t = -\min\{\mathrm{RDR}_a \times \left(wp_{rt} - wp_{r(t-1)}\right)/60 + \mathrm{RDR}_b, 0\} \tag{2.34}$$

$$\forall\, t \in \mathrm{T}, \forall b \in \mathrm{B}, \forall g \in \mathrm{G}_b, \forall r \in \mathrm{R}, \forall i \in \mathrm{Seg}_g^b, \forall\, l \in \mathrm{L}$$

The proposed model is comprised of two stages, where the on/off decisions of units are made in the first stage, and in the second stage the power reference of each generator is determined. The objective is to minimize the total costs under the worst-case realization of wind power output. The constraints listed above including minimum-up/minimum-down operation time constraints (2.14)–(2.18), start-up and shut-down cost constraints (2.19)–(2.20), system balance constraints (2.21), transmission constraints (2.22), operation cost constraints (2.23), generator capacity constraints (2.24), and the modified ramp up/down constraints (2.25)–(2.32). In constraint (2.23) the quadratic fuel cost is approximated by a p-piecewise linear function. Since DAUC involves hourly scheduling, here the intra-hour wind power variation is included in the ramp constraints of the DAUC model, in the form of (2.29)–(2.32), where total ramp reserve of all generators, each of which $\mathrm{ru}_{gt}^{b}/\mathrm{rd}_{gt}^{b}$ is defined by the maximum/minimum output and maximum ramp up/down rates as shown in (2.27)–(2.28) and (2.30)–(2.31), is forced to be no smaller than the system sub-hourly ramp requirements that are defined as a function of hourly average wind power ramp rate in (2.33)–(2.34). Note that there is a bilinear term $p_{gt}^{b} \cdot x_{gt}^{b}$ in constraints (2.28) and (2.31). Therefore, the big-M method is applied here to linearize this term, let $\rho = p_{gt}^{b} \times x_{gt}^{b}$, then we have:

$$60\mathrm{ru}_{gt}^{b} - \overline{\mathrm{PC}}_{g}^{b} \times x_{gt}^{b} + \rho \leq 0 \tag{2.35}$$

$$60\mathrm{rd}_{gt}^{b} + \overline{\mathrm{PC}}_{g}^{b} \times x_{gt}^{b} - \rho \leq 0 \tag{2.36}$$

$$\rho \leq \overline{\mathrm{PC}}_{g}^{b} \times x_{gt}^{b} \tag{2.37}$$

$$\rho \geq p_{gt}^{b} - \left(1 - x_{gt}^{b}\right)\overline{\mathrm{PC}}_{g}^{b} \tag{2.38}$$

2.7 C&CG-based Solution Methodology

The proposed improved DAUC model has a min-max-min structure, which cannot be solved directly by existing commercial optimization solvers such as CPLEX. Enumerating all the possible outcomes of the uncertain variables would lead to an extremely large-size problem and cannot be solved. Thus, in this chapter, a decomposition approach based on the Column and Constraint Generation (C&CG) method is applied. [71] To begin with, the proposed robust DAUC formulations are rewritten in a compact form for brevity as follow:

$$\min_{x} \boldsymbol{c^T x} + \max_{wp \in \mathcal{U}} \min_{y \in \mathcal{X}(y,u)} \boldsymbol{b^T y} \tag{2.39}$$

s.t. $$\mathbf{Ax} \geq \mathbf{d}, \mathbf{x} \in \boldsymbol{S_x} \tag{2.40}$$

Where, $\mathcal{X}(y,u) := \{ \mathbf{y} \in S_y : \boldsymbol{Gx} \geq \boldsymbol{h} - \boldsymbol{Ey} - \boldsymbol{M}u\}$. The main idea of the C&CG method is that, by employing a master-subproblem framework, where the subproblem identifies those uncertainty realizations that will lead to worst-case. In such way, enumerating all scenarios can be avoided. C&CG is implemented with the following procedures:

Set LB $= -\infty$, UB $= +\infty$, k $= 0$ and $\mathbf{O} = \emptyset$

Solve the following master problem (MP): derive an optimal solution $[\boldsymbol{x_{k+1}^*}, \eta_{k+1}^*, \boldsymbol{y^{1*}}, \dots, \boldsymbol{y^{k*}}]$ and update the LB $= \boldsymbol{c^T y_{k+1}^*} + \eta_{k+1}^*$.

$$\mathbf{MP}: \min_{x,\eta} \boldsymbol{c^T x} + \eta \tag{2.41}$$

s.t. $$\mathbf{Ax} \geq \mathbf{d} \tag{2.42}$$

$$\eta \geq \boldsymbol{b^T y^l}, \forall\, \mathrm{l} \in \mathbf{O} \tag{2.43}$$

$$\mathbf{Ex} + \mathbf{G}\boldsymbol{y^l} \geq \boldsymbol{h} - \boldsymbol{M}u_l^*, \forall\, \mathrm{l} \leq \mathrm{k} \tag{2.44}$$

$$\mathrm{x} \in S_x, \qquad \eta \in \mathbb{R}, \qquad y^l \in S_y, \qquad \forall\, \mathrm{l} \leq \mathrm{k}$$

Solve the following sub-problem and update the $UB = min\{UB, \boldsymbol{c^T x_{k+1}^*} + \mathcal{Q}(\boldsymbol{x_{k+1}^*})\}$. The sub-problem is as follow:

$$\textbf{SP}:\ \mathcal{Q}(\mathbf{x}) = \{\max_{wp\in\mathcal{U}} \min_{y\in\mathcal{X}(y,u)} \boldsymbol{b^T y} : \boldsymbol{Gx} \geq \boldsymbol{h} - \boldsymbol{Ey} - \boldsymbol{M}u, \mathbf{x} \in \boldsymbol{S_x}\} \tag{2.45}$$

If $UB - LB \leq \epsilon$, return $\boldsymbol{y^*_{k+1}}$ and terminate. Otherwise, create variables $\mathbf{y^{k+1}}$ and add the following constraints to the master problem **MP** (2.41)–(2.44) where u^*_{k+1} is the optimal scenario solving $\mathcal{Q}(\mathbf{x^*_{k+1}})$, update $k = k + 1$, $\mathbf{O} = \mathbf{O} \cup \{k + 1\}$ and go to step 2.

$$\boldsymbol{\eta} \geq \boldsymbol{b^T y^{l+1}} \tag{2.46}$$

$$\mathbf{Ex} + \mathbf{G}\boldsymbol{y^{k+1}} \geq \boldsymbol{h} - \boldsymbol{M}u^*_{k+1} \tag{2.47}$$

After the proposed decomposition procedure, the original DAUC formulations can be converted into a mixed-integer linear programming (MILP) problem and computed by an existing solver, such as CPLEX.

2.8 Case Study

2.8.1 Sub-hourly Wind Power Ramp Behaviors.

The aforementioned quantification method on sub-hourly wind power ramp behaviors is performed on the 2017-year data acquired from Belgium TSO ELIA. The numerical simulation results are shown in this section.

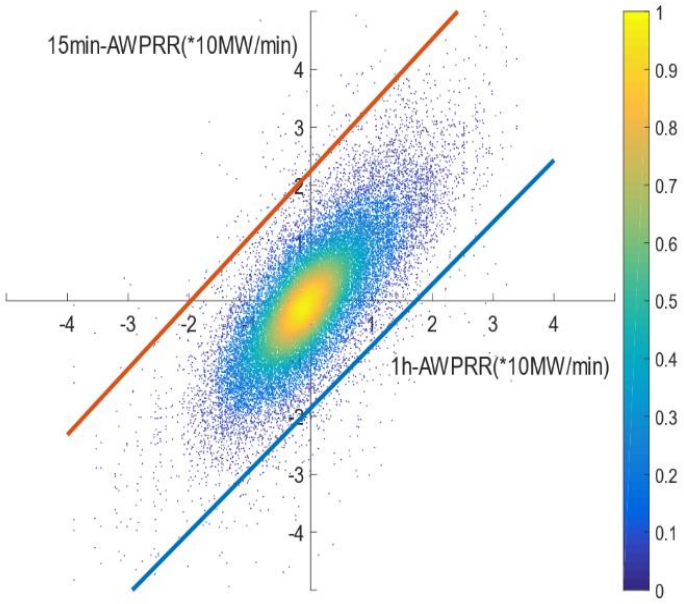

Figure 2.4 KDE results of the quantitive analysis on sub-hourly wind power ramp behaviors.

As shown in Figure 2.4, the x-axis and y-axis are the hourly average wind power ramp rate (1h-AWPRR) and the 15-minute average wind power ramp rate (15min-AWPRR), respectively. The orange line and the blue line are respectively the derived sub-hourly ramp up/down requirements $\mathcal{R}u_t/\mathcal{R}d_t$, which are linear functions of hourly average wind power ramp rate:

$$\mathcal{R}u_t = \max\{1.1405 \times \frac{\left(wp_{rt} - wp_{r(t-1)}\right)}{60} + 2.2449,0\} \tag{2.48}$$

$$\mathcal{R}d_t = -\min\{1.0725 \times \frac{\left(wp_{rt} - wp_{r(t-1)}\right)}{60} - 1.8571,0\} \tag{2.49}$$

As described before, as long as these two ramp reserve capacity constraints are imposed on the hourly ramp constraints in the UC model, the UC solutions will be able to schedule sufficient sub-hourly ramp reserves to make sure that 95% of the intra-hour ramp behaviors can be accommodated, in other words, higher utilization rate of wind power will be achieved.

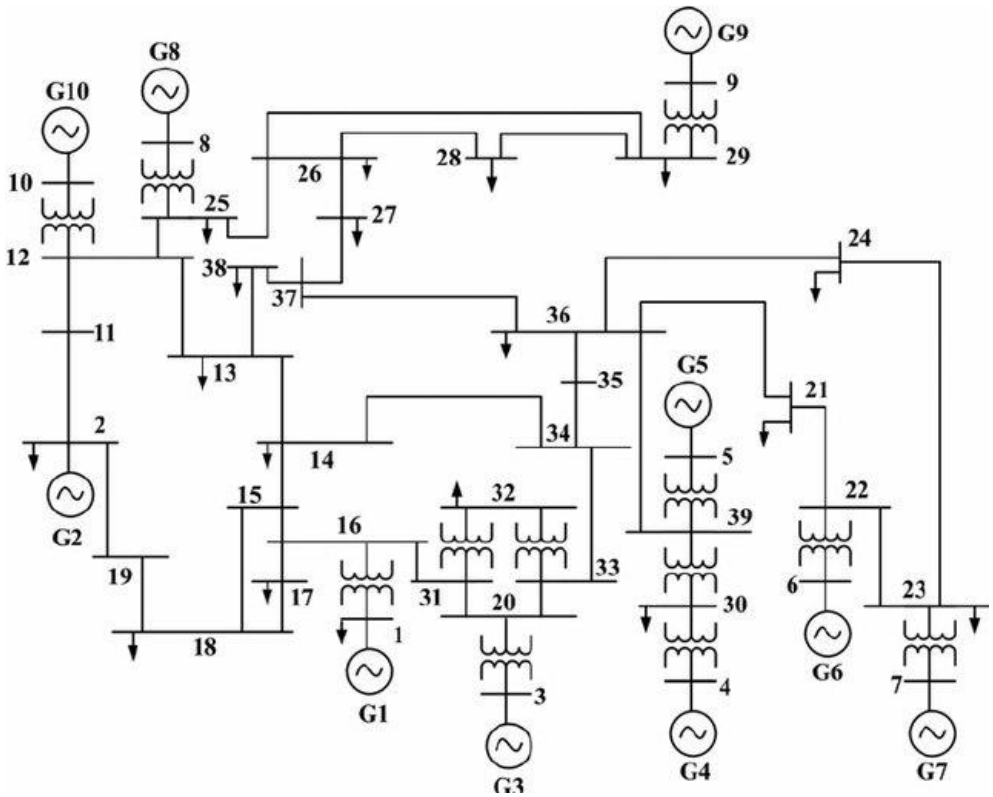

Figure 2.5 IEEE 39 Bus test system

2.8.2 Flexible UC Decisions

The aforementioned approximation method for analyzing the wind power ramp behaviors is performed on the 2017-year data acquired from Belgium TSO ELIA, which can be accessed in public database. The numerical simulation is implemented in MATLAB 2015 on a desktop with an Intel i7-6700K CPU @ 3.40 GHz and 16.0 GB RAM memory. IBM CPLEX is employed as the solver here. The numerical simulations are carried on a modified IEEE 10-generator 39-bus test system. As shown in Figure 2.5, a wind farm is connected to bus 23. The forecast value and confidential level of the forecast have been provided in Fig. 2.6.

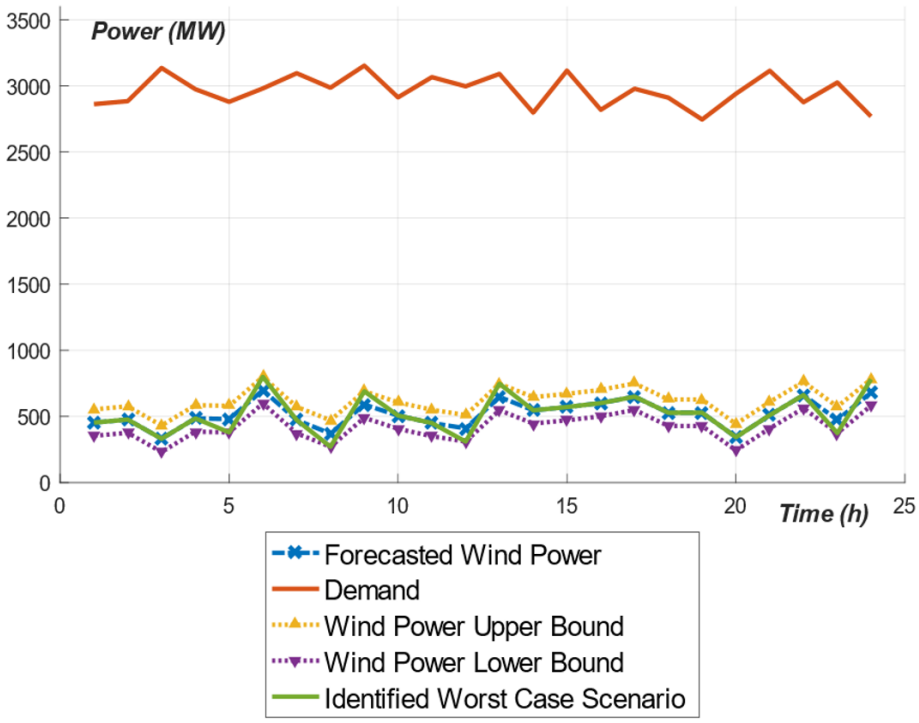

Figure 2.6 Identified worst-case wind power output

As shown in Fig. 2.6 are the confidence interval of wind power forecast value, the identified worst-case wind generation realization, and the forecasted demand.

Figure 2.7 shows the possible wind power ramp up/down range, system ramp-up reserves (RUR) and ramp-down reserves (RDR) in each operation time slot, when the model is with sub-hourly ramp constraints and without sub-hourly ramp constraints. As it is shown in Figure 2.7, the conventional UC model that neglects the sub-hourly wind ramp behaviors may not have enough ramp reserves to accommodate the sub-hourly wind power variations. It can be found in Figure 2.7 that conventional UC models cannot provide enough RUR except hour 7, 13 and 24, and cannot provide enough RDR in hour 6 and 23. In comparison our model that considers the sub-hourly ramp constraints will obtain a flexible UC solution. This solution will ensure that there are sufficient RUR and RDR to cover all possible sub-hourly wind power ramp range in each schedule period, which means that wind power can be fully utilized, and no wind curtailment or load shedding is needed.

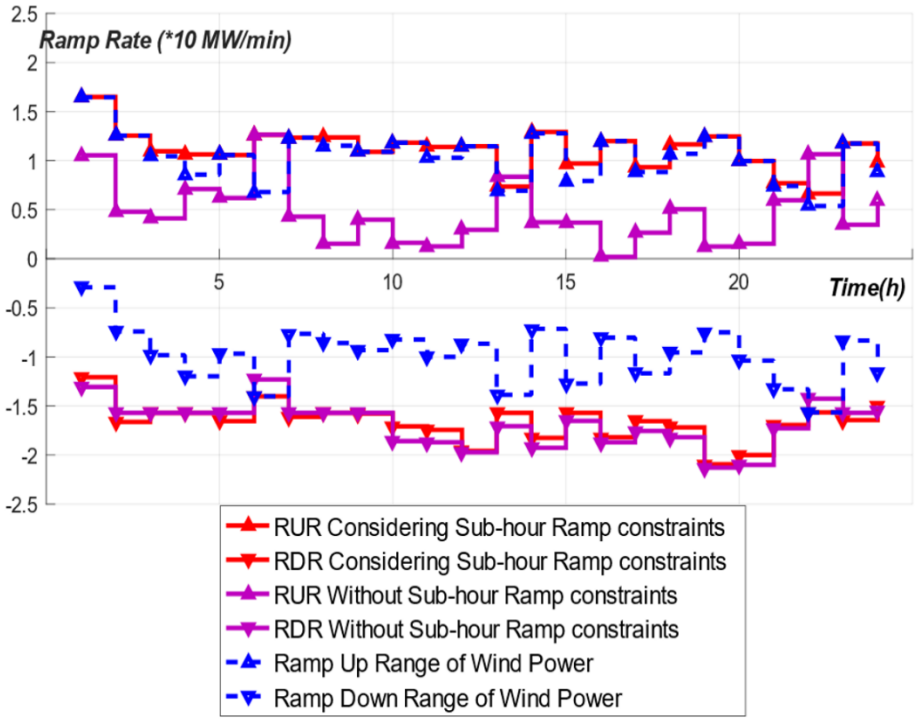

Figure 2.7 System ramp reserves and wind power ramp ranges

2.9 Conclusion

In this chapter, the most common methods for optimization under uncertainty are discussed and reviewed. In addition, an improved unit commitment model is presented to demonstrate the applications of robust optimization frameworks. This improved DAUC model is proposed to handle the uncertainty and variability of wind power output, especially in intra-hour time domains. Firstly, a non-parametric approach is developed to accurately quantify the correlation between intra-hour wind power variation and inter-hour ones. The sub-hourly operation constraints are incorporated into UC hourly operation constraints. The robust optimization is applied and the uncertain wind power is described in the form of an uncertainty set. The hourly ramp constraints in the UC model are modified to included sub-hourly ramp constraints so that the obtained robust UC solution is 'flexible' enough with sufficient ramp-up and ramp-down capacity reserves to accommodate the intra-hour wind variations. The results of case studies show the effectiveness of the proposed model, which means it will facilitate the increasing integration of wind power.

3 Price-Maker Bidding Model for Networked Microgrids under Uncertainty

3.1 Abstract

A price-maker bidding strategy for networked microgrids (NMGs) in the day-ahead electricity market considering uncertainty is proposed in this chapter. The objective of the proposed model is to maximize the net revenue by coordinating individual microgrids in the NMGs to determine hourly supply and demand price-quota bidding curves. A hybrid stochastic-robust optimization method is developed to manage multiple uncertainties. The bidding problem is originally presented as a hard-to-solve mixed-integer nonlinear problem (MINLP), which is later converted to its easy-to-solve mixed integer linear problem counterpart (MILP). To protect the privacy of each microgrid (MG) and improve the scalability of the bidding model as well, a semi-decentralized optimization framework based on Dantzig-Wolfe decomposition (DWD) is used to obtain global optimality. Numerical simulations based on real-world data are presented to validate the proposed bidding model. It has been found that the proposed price-maker bidding model outperforms the existing price-taker ones.

3.2 Nomenclature

Superscripts:

ESS	Energy Storage Systems.
CG	Controllable Generator
RG	Renewable Generator
DL	Deferrable Load.
CL	Critical Load.

min/max Minimum/maximum value of a quota

Indices and sets:

t/T Schedule time horizon.

m/M Index/set of microgrids.

k/Θ Index/set of stochastic market scenarios.

g/G^{m} Index/sets of CGs in MG m.

e/E^{m} Index/sets of RGs in MG m.

r/R^{m} Index/sets of ESSs in MG m.

s/S Number of segments of the purchase bid price quota curve.

l/L Number of segments of sell bid price quota curve.

Parameters:

$\mathrm{L}^{\mathrm{INT}}_{mj,\max}$ Max transmission capacity between MG m and MG j

$\mathrm{L}^{\mathrm{EX}}_{m,\max}$ Max transmission capacity between MG m and the utility grid.

$\epsilon^{\mathrm{CG}}_{g}$ Per unit production cost of CG g. ($/MWh)

$\mathrm{P}^{\mathrm{CG}}_{g,\max}$ Max output of CG g.

$\mathrm{P}^{\mathrm{CG}}_{g,\min}$ Min output of CG g.

$\mathrm{R}^{\mathrm{CG,U}}_{g,\max}$ Max upward ramp rate of CG g.

$\mathrm{R}^{\mathrm{CG,D}}_{g,\max}$ Max downward ramp rate of CG g.

$P^{\mathrm{RG,F}}_{r,t}$ Renewable generation forecast value of r

$\mathrm{SOC}^{\mathrm{ESS}}_{e,\min}$ Max state of charge of ESS e.

$\mathrm{SOC}_{e,\max}^{\mathrm{ESS}}$ Min state of charge of ESS e.

$\mathrm{P}_{e,\max}^{\mathrm{Dis,ESS}}$ Max discharging power of ESS e.

$\mathrm{P}_{e,\max}^{\mathrm{Ch,ESS}}$ Max charging power of ESS e

$\eta_{e,c}^{\mathrm{ESS}}$ Charging efficiency of ESS e.

$\eta_{e,d}^{\mathrm{ESS}}$ Discharging efficiency of ESS e

$\mathrm{C}_{e,\max}^{\mathrm{ESS}}$ Max capacity of ESS e

σ_e^{ESS} Per unit degradation cost of ESS e. ($/MWh)

$\mathrm{D}_m^{\mathrm{DL}}$ Total amount of deferrable load of MG m.

$\mathrm{D}_{m,\min}^{\mathrm{DL}}$ Min serving rate for DL of MG m.

$\mathrm{D}_{m,\max}^{\mathrm{DL}}$ Max serving rate for DL of MG m.

$\mathrm{D}_m^{\mathrm{CL,F}}$ Critical load forecast value of MG m.

$\mathrm{T}_m^{\mathrm{S}}$ Start time to serve deferrable load.

$\mathrm{T}_m^{\mathrm{E}}$ End time to serve deferrable load.

Decision Variables:

$p_{mj,t}^{\mathrm{INT}}$ Energy transaction between microgrid m and j. (+: from m to j, -: from j to m)

$f_{m,t}^{\mathrm{OP}}$ Total operation cost of MG m.

$p_{m,t}^{\mathrm{ES}}$ Total energy sold to market by MG m.

$p_{m,t}^{\mathrm{EB}}$ Total energy bought from market by MG m.

$u_{g,t}^{\mathrm{CG}}$ Binary variables indicating the on/off status of CG g.

$p_{g,t}^{\mathrm{CG}}$ Power reference of CG g.

$p_{r,t}^{\mathrm{RG}}$	Output of RG r.
$x_{e,t}^{\mathrm{ESS}}$	Binary variables indicating the charging status of ESS e.
$y_{e,t}^{\mathrm{ESS}}$	Binary variables indicating the discharging status of ESS e.
$p_{e,t}^{\mathrm{Ch,ESS}}$	Charging power of ESS e at time t.
$p_{e,t}^{\mathrm{Dis,ESS}}$	Discharging power of ESS e at time t.
$c_{e,t}^{\mathrm{ESS}}$	Energy storage level of ESS e at time t.
$p_{e,t}^{\mathrm{E,ESS}}$	Net output of ESS e at time t.
$d_{m,t}^{\mathrm{CL}}$	Critical load of MG m at time t.
$d_{m,t}^{\mathrm{DL}}$	Deployed deferrable load at time slot t.
$p_{m,t}^{\mathrm{NET}}$	Net power generation of the MG m.
$z_{m,t}^{\mathrm{EX+}}$	Binary variables indicating that microgrid m is selling energy to market.
$z_{m,t}^{\mathrm{EX-}}$	Binary variables indicating that microgrid m is purchasing energy from market.
$p_{k,t}^{\mathrm{DS}}$	Cleared supply energy quota at time slot t in scenario k.
$p_{k,t}^{\mathrm{DB}}$	Clear purchased energy quota at time slot t in scenario k.
$v_{k,s,t}^{\mathrm{DB}}$	Indicate whether the intersection is located on segment s of purchase bid curve for period t in scenario k.
$a_{k,s,t}^{\mathrm{DB}}$	Horizontal length between the intersection point and the starting point of purchase bid curve segment s for period t in scenario k.
$b_{k,s,t}^{\mathrm{DB}}$	Vertical length between the intersection and the starting point of demand bidding curve segment s for period t in scenario k.
$v_{k,l,t}^{\mathrm{DS}}$	Indicate whether the intersection is located on segment l of supply bidding curve for period t in scenario k.

$a_{k,l,t}^{\mathrm{DS}}$ Horizontal length between the intersection and the starting point of sell bid curve segment l for period t in scenario k.

$b_{k,l,t}^{\mathrm{DS}}$ Vertical length between the intersection and the starting point of sell bid curve segment l for period t in scenario k.

3.3 Introduction

In the context of deregulated electricity markets, microgrids generally act as prosumers because they can submit either supply offers or demand bids. In recent years, a considerable amount of studies on the bidding models for microgrids have been carried out to maximize their revenue from the market [29], [30], [72], [73]. Considering that there will be multiple microgrids in the system, the concept of networked microgrids (NMGs) has attracted much attention in recent years. The NMGs refers to a collaboration framework that multiple electrical neighboring microgrids are networked and coordinated as a single dispatchable unit [74]. This collaboration can greatly improve the performance of individual microgrids, as it can better mitigate demand and generation uncertainties and promote economic benefits, etc [75]–[77]. When participating in the electricity market, however, bidding model for an NMGs entity should be different from bidding model for a single microgrid in [75]–[77]. The reason is that, by coordinating generation and demand of individual microgrids, the NMGs will have a large aggregated capacity to influence the market-clearing prices. Comparing with price-taker biding models in [75]–[77], price-maker bidding models are more appropriate for NMGs. To be specific, the price-maker bidding model for NMGs can compile price-quota bids for both supply and demand to maximize the NMGs' revenue from the market [78]–[80]

Another problem that needs to be addressed is the coordination framework for the NMGs. Existing coordination methods can be summarized into three categories: centralized, decentralized and semi-decentralized. In the centralized coordination framework, there is one central coordinator that schedules the operations of all microgrids, based on detailed information of each involving microgrid, to achieve optimum. However, this framework also brings privacy concerns and high computation burdens [33], [81], [82]. The decentralized ones can avoid the drawbacks of centralized ones. In such a framework the central coordinator is no longer needed. Instead, the

local coordinator at each microgrid solves the bidding problem by sharing information other MLCs [15],[16]. However, a decentralized framework also suffers from following drawbacks: i) it relies heavily on the communications between individual microgrids, ii) it may violate the physical constraints of the network between individual microgrids [85].

A third type can be referred to as the semi-decentralized framework, which is a hybrid of the first two categories [85]–[87]. There is one network central coordinator (NCC) and multiple self-owned microgrid local coordinators (MLC) in such a framework. Neither the NCC nor the MLC needs to have detailed information about the NMGs configuration to solve the scheduling problem. In [85] an energy transaction model between microgrids is solved base on KKT conditions. A distributed direct energy trading mechanism considering AC power flow constrains is solved based on alternative direction method of multipliers (ADMM) in [86]. An algorithm based on sub-gradient method is proposed in [19] to optimize the energy transactions problem between individual microgrids. However, a common problem of these methods is that none of them is able to solve bidding models with integer (binary) decision variables, i.e. the on/off status of generators, the charging/discharging of energy storage systems, etc.

Among existing studies, it can be observed that the research gap exists in price-maker bidding models for NMGs. In this chapter, a price-maker bidding model for a networked microgrids entity in the day-ahead pool-based electricity market is proposed.

Main contributions of this research are summarized as follow:

Considering that an NMGs entity has an aggregated capacity that is large enough to influence the market-clearing prices, a price-maker day-ahead bidding strategy for the NMGs entity is proposed. All microgrids in the NMGs are coordinated cooperatively to submit aggregated price-quota bids for each hour of next day. These bids specify the energy and the corresponding price that the NMGs would like to supply or purchase.

Uncertainty sources in the bidding model are discussed and managed using a hybrid stochastic-robust optimization framework. The bidding model is originally formulated into a mixed-integer non-linear problem (MINLP). To reduce the computation burdens, the MINLP is then reformulated into its mixed-integer linear problem (MILP) counterpart.

To protect the privacy of each microgrid, and enhance the scalability of the bidding model as well, the NMGs are coordinated by a semi-decentralized framework. The Dantzig-Wolfe decomposition (DWD) is employed to optimize the collaboration between individual microgrids. By exchanging necessary information between the NCC and MLCs iteratively, the bidding problem can be solved to global optima.

The rest of this chapter is organized as follows. Section II describes the basic setups of the model. Section III presents the detailed formulations of the price-maker bidding model. Reformulation methods and the solution algorithm are presented in section IV. Section V conducts numerical simulations based on real-world data. Finally, in section VI the chapter is concluded.

3.4 Modeling Approach

A. Coordination Framework

As shown in Figure 3.1, a semi-decentralized coordination framework for NMGs. In such a framework the NCC and LMCs have different duties. The NCC is responsible for scheduling the energy transactions between individual microgrids, and interacting with the market operator by submitting aggregated bids as well. While MLCs are responsible for scheduling energy sources within their individual control area according to the information received from NCC. The clear bids are delivered by microgrids that have interconnection with the utility grid (UG). Information can be exchanged through bi-directional communications between MLCs and NCC.

B. Microgrid Components

Each self-governing microgrid of the NMGs may consist of following energy sources, including controllable generators (CG), renewable generators (RG), deferrable loads (DL), critical loads (CL), and energy storage systems (ESS), etc [88]. Controllable generators include micro-turbines, fuel-cells, and diesel generators. Renewable generators include wind turbines and solar panels. Deferrable loads, a.k.a. time-shiftable loads, are these loads that require specific time periods to be satisfied, but can be served any time within this period. Examples of deferrable loads including plug-in electric vehicles, irrigation pumps, etc. Opposite to deferrable loads are critical loads that must be satisfied with the exact amount at exact time. ESSs in this chapter are assumed to be battery energy storage systems.

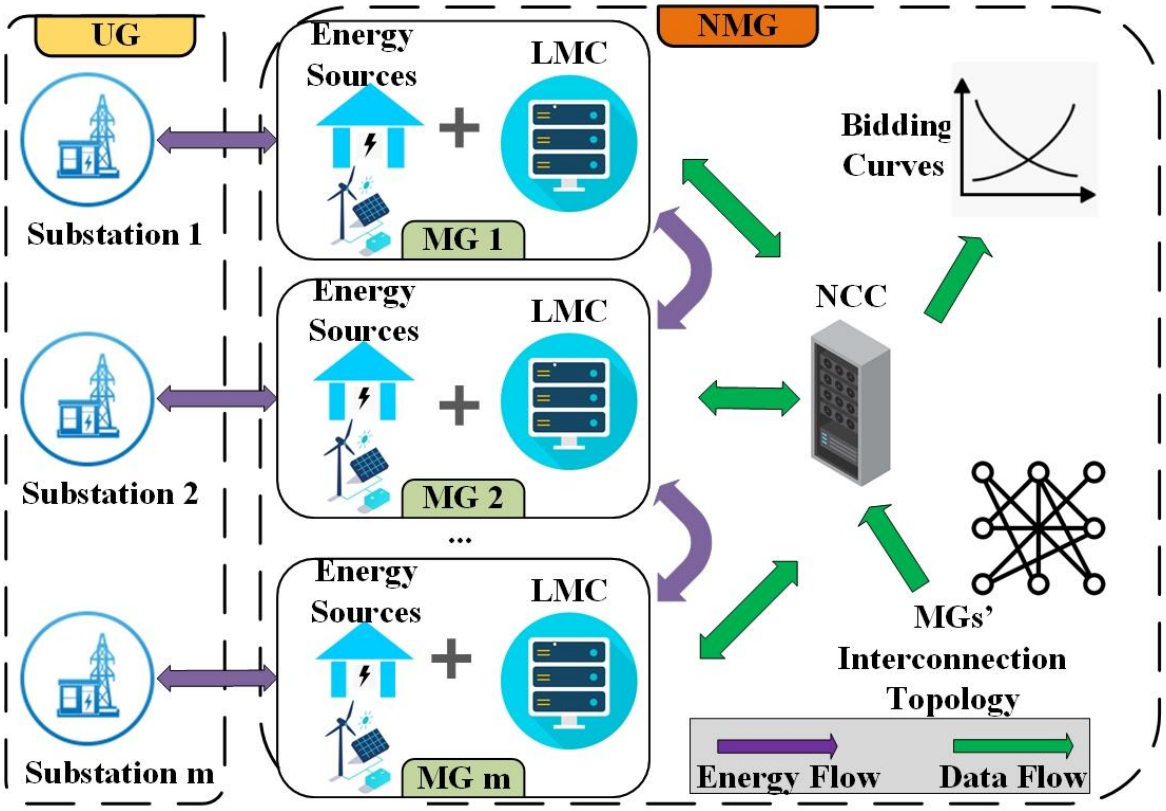

Figure 3.1 Semi-decentralized coordination framework of the NMGs

C. Day-Ahead Market Model

In the day-ahead market, the market operators collect bids from all participants and clear the market for each hour of the next day [60], [89], [90]. The influence of price-maker participants on the spot price can be modeled using residual supply/demand curves, as illustrated in Figure 3.2, which can be obtained by forecast or from historical data [91]. Generally, there are price-taker entities and price-maker entities.

When the price bids of a participant are zeros, it is called a price taker. A price-taker entity cannot affect the pool prices. It will accept the market-clearing prices whatever it is. It is the ISO's responsibility to determine the price and capacity that is going to be sold to the market by a price-taker entity. This decision making procedure is made based on the principals that aim at minimizing the market-clearing prices. However, being price-takers do not mean that they receive zero payments because every participant is cleared at the same price as other market participants.

For a price-maker NMGs entity, it can either purchase or supply electricity by submitting price-quota bidding curves to the day-ahead market. The price-quota bidding curves are stepwise curves that are comprised of multiple price value and energy quota pairs. These curves indicate that the NMGs will purchase (supply) the submitted energy quota only if the market-clearing price is no higher (lower) than the submitted price. In terms of purchase bids, the price-quota curves are stepwise monotonically increasing, while in terms of supply bids they are stepwise monotonically decreasing [32]. As shown in Figure 3.2, the price and corresponding quota are cleared at intersection points between the market residual supply/demand curves and NMGs' price-quota offering/bidding curves.

D. Hybrid Optimization Model

There are multiple uncertainties that need to be considered in the bidding model. In general, these uncertainties can be summarized into two categories: i) external uncertainties and, ii) internal uncertainties. The external uncertainties refer to the uncertain market residual supply/demand curves, while the internal uncertainties refer to the uncertain generations and demands of each microgrid. In this chapter, these uncertainties are managed by a hybrid stochastic-robust optimization framework. The scenario-based stochastic optimization method is used to manage the uncertainty of residual supply/demand curves on day-ahead market, while the uncertainty sets based robust optimization method is used to manage uncertainties of generation and demand. This hybrid optimization framework guarantees: i) the submitted supply offers/demand bids capacity can be delivered under the worst-case realizations, ii) expected total revenue can be maximized.

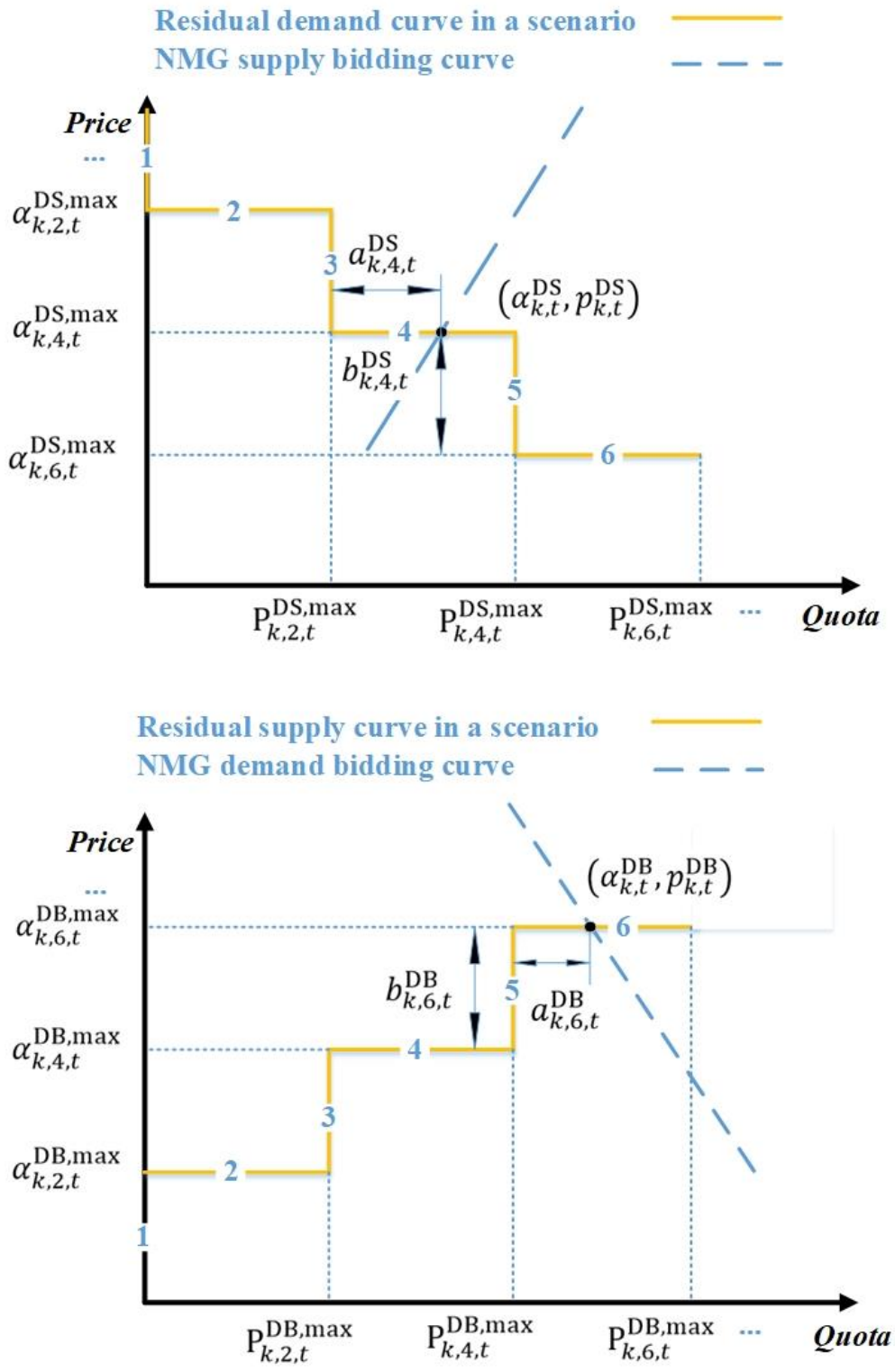

Figure 3.2 Market residual supply/demand price-quota curves

3.5 Model Formulation

We consider an NMGs entity that participates in the day-ahead market as a price-maker to maximize its total revenue while subject to physical constraints and market rules. The constraints and objective function are presented sequentially in this section. The objective function of the bidding model is to maximize expected total revenue by determining price-quota supply/demand bidding curves for each hour of the next day. This model subjects to physical constraints of all energy sources inside the NMGs and the interconnection network among each microgrid. It should be noted that the reactive power balance constraints and active power losses are neglected here, this is because that, i) it is a common practice for day-ahead schedule problems, and ii) linearization methods for calculating active power losses and reactive power flow can be found in existing studies, which means that the complexity of the model will not be affected [25]-[26].

3.5.1 Controllable Generators Constraints

$$\mathrm{P}_{g,\min}^{\mathrm{CG}} \times u_{k,g,t}^{\mathrm{CG}} \le p_{k,g,t}^{\mathrm{CG}} \le P_{g,\max}^{\mathrm{C}} \times u_{k,g,t}^{\mathrm{CG}} \tag{3.1}$$

$$p_{k,g,t}^{\mathrm{CG}} - p_{k,g,t-1}^{\mathrm{CG}} \le \mathrm{R}_{g,\max}^{\mathrm{CG,U}} \times u_{k,g,t-1}^{\mathrm{CG}} + \mathrm{P}_{g,\max}^{\mathrm{CG}} \times \left(1 - u_{k,g,t}^{\mathrm{CG}}\right) \tag{3.2}$$

$$p_{k,g,t-1}^{\mathrm{CG}} - p_{k,g,t}^{\mathrm{CG}} \le \mathrm{R}_{g,\max}^{\mathrm{CG,D}} \times u_{k,g,t}^{\mathrm{CG}} + \mathrm{P}_{g,\max}^{\mathrm{CG}} \times \left(1 - u_{k,g,t-1}^{\mathrm{CG}}\right) \tag{3.3}$$

$$f_{k,g,t}^{\mathrm{CG}} = p_{k,g,t}^{\mathrm{CG}} \times \epsilon_{g}^{\mathrm{CG}} \times 1h \tag{3.4}$$

$$f_{k,g,t}^{\mathrm{CG}}, p_{k,g,t}^{\mathrm{CG}} \ge 0, u_{k,g,t}^{\mathrm{CG}} \in \{0,1\} \tag{3.5}$$

The output limits of CGs are described by (3.1). Ramp constraints are enforced by (3.2)-(3.3). The generation costs are approximated by (3.4). It should be noted that, in the cases of quadratic generation cost functions, they can be easily linearized using piecewise linear functions [35], which does not affect the complexity of the model. This piecewise linearization technique also works for calculating ESS degradation costs.

3.5.2 Energy Storage Systems Constraints

$$-1 \times x_{k,e,t}^{\mathrm{ESS}} \times \mathrm{P}_{e,\max}^{\mathrm{Ch,ESS}} \leq p_{k,e,t}^{\mathrm{Ch,ESS}} \leq 0 \tag{3.6}$$

$$0 \leq p_{k,e,t}^{\mathrm{Dis,ESS}} \leq y_{k,e,t}^{\mathrm{ESS}} \times \mathrm{P}_{e,\max}^{\mathrm{Dis,ESS}} \tag{3.7}$$

$$c_{k,e,t}^{\mathrm{ESS}} = c_{k,e,t-1}^{\mathrm{ESS}} + \left(p_{k,e,t}^{\mathrm{Ch,ESS}} \eta_e^{\mathrm{Ch,ESS}} - p_{k,e,t}^{\mathrm{Dis,ESS}} / \eta_e^{\mathrm{Dis,ESS}}\right) \times 1h \tag{3.8}$$

$$\mathrm{SOC}_{e,\min}^{\mathrm{ESS}} \times \mathrm{C}_e^{\mathrm{ESS}} \leq c_{k,e,t}^{\mathrm{ESS}} \leq \mathrm{SOC}_{e,\max}^{\mathrm{ESS}} \times \mathrm{C}_e^{\mathrm{ESS}} \tag{3.9}$$

$$f_{k,e,t}^{\mathrm{ESS}} \geq \left(c_{k,e,t}^{\mathrm{ESS}} - c_{k,e,t-1}^{\mathrm{ESS}}\right) \times \sigma_e \tag{3.10}$$

$$f_{k,e,t}^{\mathrm{ESS}} \geq \left(c_{k,e,t-1}^{\mathrm{ESS}} - c_{k,e,t}^{\mathrm{ESS}}\right) \times \sigma_e \tag{3.11}$$

$$0 \leq x_{k,e,t}^{\mathrm{ESS}} + y_{k,e,t}^{\mathrm{ESS}} \leq 1 \tag{3.12}$$

$$\mathrm{C}_{e,ini}^{\mathrm{ESS}} = c_{k,e,T}^{\mathrm{ESS}} \tag{3.13}$$

$$x_{k,e,t}^{\mathrm{ESS}}, y_{k,e,t}^{\mathrm{ESS}} \in \{0,1\}, c_{k,e,t}^{\mathrm{ESS}}, p_{k,e,t}^{\mathrm{Ch,ESS}}, p_{k,e,t}^{\mathrm{Dis,ESS}}, f_{k,e,t}^{\mathrm{ESS}} \geq 0 \tag{3.14}$$

Constraints (3.6)-(3.9) describe the power and energy limits of ESSs. (3.10) and (3.11) are linear functions for approximating ESSs' degradation costs. It enforced by (3.12) that each ESS cannot charge and discharge at the same time. (3.13) enforces that the energy stored in the ESS of each MG remains the same as the initial storage level $\mathrm{C}_{e,ini}^{\mathrm{ESS}}$, so that no free energy is used within the scheduling horizon.

3.5.3 Deferrable Loads Constraints

$$\sum_{t=T_m^{\mathrm{S}}}^{T_m^{\mathrm{E}}} d_{k,m,t}^{\mathrm{DL}} = \mathrm{D}_m^{\mathrm{DL}}, \forall t \in [\mathrm{T}_m^{\mathrm{S}}, \mathrm{T}_m^{\mathrm{E}}] \tag{3.15}$$

$$\mathrm{D}_{m,\min}^{\mathrm{DL}} \leq d_{k,m,t}^{\mathrm{DL}} \leq \mathrm{D}_{m,\max}^{\mathrm{DL}}, \forall t \in [\mathrm{T}_m^{\mathrm{S}}, \mathrm{T}_m^{\mathrm{E}}] \tag{3.16}$$

$$d_{k,m,t}^{\mathrm{DL}} = 0, \forall t \notin [\mathrm{T}_m^{\mathrm{S}}, \mathrm{T}_m^{\mathrm{E}}] \tag{3.17}$$

Constraint (3.15) represents the total required electricity amount of deferrable loads, (3.16) represents the minimum and maximum serve rate of deferrable demand in each hour. (3.17) represents the start and end time to satisfy deferrable loads.

3.5.4 Transmission Capacity Constraints:

$$0 \le p_{k,m,t}^{\mathrm{ES}} \le \theta_t \mathrm{L}_{m,\max}^{\mathrm{EX}} \tag{3.18}$$

$$0 \le p_{k,m,t}^{\mathrm{EB}} \le (1-\theta_t)\mathrm{L}_{m,\max}^{\mathrm{EX}} \tag{3.19}$$

$$-\mathrm{L}_{mj,\max}^{\mathrm{INT}} \le p_{k,mj,t}^{\mathrm{INT}} \le \mathrm{L}_{mj,\max}^{\mathrm{INT}}, m \ne j \tag{3.20}$$

(3.18) and (3.19) describe the transmission capacity limits on energy transactions between each MG and the utility grid, while (3.20) describes the transmission capacity limits on energy transactions between individual microgrids inside the NMG cluster.

3.5.5 Generation-Demand Balance Constraints

$$p_{k,m,t}^{\mathrm{NET}} = \sum_{g \in \mathrm{G}^m} p_{k,g,t}^{\mathrm{CG}} + \sum_{e \in \mathrm{E}^m} \left(p_{k,e,t}^{\mathrm{Dis,ESS}} - p_{k,e,t}^{\mathrm{Ch,ESS}}\right) + \sum_{r \in \mathrm{R}^m} p_{r,t}^{\mathrm{RG}} - \left(d_{k,m,t}^{\mathrm{DL}} + d_{m,t}^{\mathrm{CL}}\right) \tag{3.21}$$

$$p_{k,m,t}^{\mathrm{NET}} + \sum_{j \in M, j \ne m} p_{k,mj,t}^{\mathrm{INT}} - p_{k,m,t}^{\mathrm{ES}} + p_{k,m,t}^{\mathrm{EB}} = 0 \tag{3.22}$$

$$p_{k,mj,t}^{\mathrm{INT}} + p_{k,jm,t}^{\mathrm{INT}} = 0, m \ne j \tag{3.23}$$

(3.21) represents the generation-demand balance constraints within each MG. (3.22) represents the generation-demand balance constraints of the whole NMGs. (3.23) describes that, for the energy transactions between microgrid m and j, the energy exported from microgrid j to m equals to the energy imported by m from j.

3.5.6 Market Residual Supply and Demand Price-Quota Curves

The uncertainties of the day-ahead market are managed by a 2-stage stochastic optimization framework. Firstly, K scenarios of residual supply/demand price-quota curves are generated from historical data, with each assigned with a probability ς_k. Each scenario contains market residual supply and demand price-quota curves for 24 hours of the day. It has been illustrated in section II-C that for price-makers both supply offers and demand bids are submitted in the form of multiple price-quota pairs, i.e. $\left(p_{k,t}^{\mathrm{DS}}, \alpha_{k,t}^{\mathrm{DS}}\right)$ and $\left(p_{k,t}^{\mathrm{DB}}, \alpha_{k,t}^{\mathrm{DB}}\right)$. In terms of supply bidding curve, for hour t in scenario k, it is formulated into a step-wise increasing curve with L segments. Each segment is marked by two pairs of endpoints that are respectively $\left(p_{k,s,t}^{\mathrm{DS,min}}, \alpha_{k,s,t}^{\mathrm{DS,min}}\right)$ and $\left(p_{k,s,t}^{\mathrm{DS,max}}, \alpha_{k,s,t}^{\mathrm{DS,max}}\right)$. For each vertical segment, $p_{k,s,t}^{\mathrm{DS,min}} = p_{k,s,t}^{\mathrm{DS,max}}$, while for each horizontal segment, $\alpha_{k,s,t}^{\mathrm{DS,min}} = \alpha_{k,s,t}^{\mathrm{DS,max}}$. Similarly, the demand bidding curve for hour t in scenario k can be formulated into a step-wise decreasing curve with L segments. Each segment of the residual demand curve is marked by two pairs of endpoints, that are respectively $\left(p_{k,l,t}^{\mathrm{DB,min}}, \alpha_{k,l,t}^{\mathrm{DB,min}}\right)$ and $\left(p_{k,l,t}^{\mathrm{DB,max}}, \alpha_{k,l,t}^{\mathrm{DB,max}}\right)$. For each vertical segment, $p_{k,l,t}^{\mathrm{DB,min}} = p_{k,l,t}^{\mathrm{DB,max}}$, while for each horizontal segment, $\alpha_{k,l,t}^{\mathrm{DB,min}} = \alpha_{k,l,t}^{\mathrm{DB,max}}$.

3.5.7 Uncertain Critical Load and Renewable Generation:

The uncertainties of both renewable generation and critical loads are formulated using uncertainty set:

$$\begin{gathered} \mathrm{P}_{r,t}^{\mathrm{RG,F}} - \gamma_{r,t}^{\mathrm{L}} \overline{\mathrm{P}}_{r,t}^{\mathrm{L}} \leq p_{r,t}^{\mathrm{E,RG}} \leq \mathrm{P}_{r,t}^{\mathrm{RG,F}} + \gamma_{r,t}^{\mathrm{U}} \overline{\mathrm{P}}_{r,t}^{\mathrm{U}} \\ \gamma_{r,t}^{\mathrm{L}}, \gamma_{r,t}^{\mathrm{U}} \in [0, \Gamma_{r,t}^{\mathrm{RG}}] \end{gathered} \tag{3.24}$$

$$\begin{gathered} \mathrm{D}_{m,t}^{\mathrm{CL,F}} + \varepsilon_{m,t}^{\mathrm{U}} \overline{\mathrm{D}}_{m,t}^{\mathrm{U}} \leq d_{m,t}^{\mathrm{CL}} \leq \mathrm{D}_{m,t}^{\mathrm{CL,F}} - \varepsilon_{m,t}^{\mathrm{L}} \overline{\mathrm{D}}_{m,t}^{\mathrm{L}} \\ \varepsilon_{m,t}^{\mathrm{L}}, \varepsilon_{m,t}^{\mathrm{U}} \in [0, \Gamma_{m,t}^{\mathrm{CL}}] \end{gathered} \tag{3.25}$$

Uncertainties of RG generations are modeled by using an uncertainty set as described in (3.24), where $\overline{\mathrm{P}}_{r,t}^{\mathrm{RG,L}}$ and $\overline{\mathrm{P}}_{r,t}^{\mathrm{RG,U}}$ are respectively lower bounds and upper bounds of the renewable generation forecast value. $\gamma_{r,t}^{\mathrm{L}}$ and $\gamma_{r,t}^{\mathrm{U}}$ are respectively the deviation from lower and upper bound.

Values of $\overline{\mathrm{P}}_{r,t}^{\mathrm{RG,L}}$ and $\overline{\mathrm{P}}_{r,t}^{\mathrm{RG,U}}$ can be obtained from fothe recast or historical data. $\Gamma_{r,t}^{\mathrm{RG}}$ is the uncertainty budget that controls the conservativeness. Uncertainties of critical loads are modeled in a similar way as shown in (3.25).

3.5.8 Profit Function

The complete bidding model is formulated as follow:

$$\max \min \sum_{k\in\Theta}^{\mathrm{K}} \varsigma_k \sum_{t=1}^{\mathrm{T}} \left(p_{k,t}^{\mathrm{DS}} \times \alpha_{k,t}^{\mathrm{DS}} - p_{k,t}^{\mathrm{DB}} \times \alpha_{k,t}^{\mathrm{DB}} - f_{k,t}^{OP}\right) \tag{3.26}$$

s.t. (3.1)-(3.25)

$$f_{k,m,t}^{\mathrm{OP}} = \sum\nolimits_{e\in \mathrm{E}^m} f_{k,e,t}^{\mathrm{DE}} + \sum\nolimits_{g\in \mathrm{G}^m} f_{k,g,t}^{\mathrm{GEN}} \tag{3.27}$$

$$p_{k,t}^{\mathrm{DS}} = \sum\nolimits_{m=1} p_{k,m,t}^{\mathrm{ES}} \tag{3.28}$$

$$p_{k,t}^{\mathrm{DB}} = \sum\nolimits_{m=1} p_{k,m,t}^{\mathrm{EB}} \tag{3.29}$$

$$f_{k,t}^{\mathrm{OP}} = \sum\nolimits_{m=1} f_{k,m,t}^{\mathrm{OP}} \tag{3.30}$$

$$\forall k \in \Theta, t \in \mathrm{T}, m \in \mathrm{M}, j \in \mathrm{M}, g \in \mathrm{G}^m, r \in \mathrm{R}^m, e \in \mathrm{E}^m$$

(3.26) is the objective function that maximizes the expected total revenue from the day-ahead market, where $p_{k,t}^{\mathrm{DS}} \times \alpha_{k,t}^{\mathrm{DS}}$ is the revenue from selling electricity, $p_{k,t}^{\mathrm{DB}} \times \alpha_{k,t}^{\mathrm{DB}}$ is the revenue from purchasing electricity, $f_{k,t}^{OP}$ is the total operation cost. Constraints (3.27) and (3.28) represents that the bid for each hour is the aggregation of all microgrids. (3.30) describes the total operation cost for each hour.

3.6 Solution Methodology

The bidding problem is originally formulated into a hard-to-solve mixed-integer nonlinear problem (MINLP). In this section, firstly a MILP counterpart of the bidding problem is derived.

Then the Dantzig-Wolfe decomposition algorithm is employed to solve this MILP counterpart in a semi-decentralized manner.

3.6.1 MILP Counterpart of the Bidding Model

1 Derive the Robust Counterpart

Based on strong duality theory [93], by introducing dual and auxiliary variables, constraints corresponding to uncertain renewable generation (3.24) and demand (3.25) in the original revenue optimization model are reformulated:

$$\max \sum_{k\in\Theta}^{\mathrm{K}} \varsigma_k \sum_{t=1}^{\mathrm{T}} \left(p_{k,t}^{\mathrm{DS}} \times \alpha_{k,t}^{\mathrm{DS}} - p_{k,t}^{\mathrm{DB}} \times \alpha_{k,t}^{\mathrm{DB}} - f_{k,t}^{OP}\right) \tag{3.31}$$

s.t. (3.1)-(3.23)&(3.27)-(3.30)

$$p_{r,t}^{\mathrm{RG}} + \lambda_{r,t}^{\mathrm{RG}}\Gamma_{r,t}^{\mathrm{RG}} + \mu_{r,t}^{\mathrm{RG}} - \left(\overline{\mathrm{P}}_{r,t}^{\mathrm{L}} + \underline{\mathrm{P}}_{r,t}^{\mathrm{U}}\right)/2 \le 0 \tag{3.32}$$

$$\lambda_{r,t}^{\mathrm{RG}} + \mu_{r,t}^{\mathrm{RG}} + \varrho_{r,t}^{\mathrm{RG}} \times \left(\overline{\mathrm{P}}_{r,t}^{\mathrm{L}} + \underline{\mathrm{P}}_{r,t}^{\mathrm{U}}\right)/2 \ge 0 \tag{3.33}$$

$$d_{m,t}^{\mathrm{CL}} + \lambda_{m,t}^{\mathrm{CL}}\Gamma_{m,t}^{\mathrm{CL}} + \mu_{m,t}^{\mathrm{CL}} - \left(\overline{\mathrm{D}}_{m,t}^{\mathrm{L}} + \underline{\mathrm{D}}_{m,t}^{\mathrm{U}}\right)/2 \le 0 \tag{3.34}$$

$$\lambda_{m,t}^{\mathrm{CL}} + \mu_{m,t}^{\mathrm{CL}} + \varrho_{m,t}^{\mathrm{CL}} \times \left(\overline{\mathrm{D}}_{m,t}^{\mathrm{L}} + \underline{\mathrm{D}}_{m,t}^{\mathrm{U}}\right)/2 \ge 0 \tag{3.35}$$

$$\varrho_{m,t}^{\mathrm{CL}}, \varrho_{r,t}^{\mathrm{RG}} \ge 1, \lambda_{m,t}^{\mathrm{CL}}, \mu_{m,t}^{\mathrm{CL}}, \lambda_{r,t}^{\mathrm{RG}}, \mu_{r,t}^{\mathrm{RG}} \ge 0 \tag{3.36}$$

where, $\lambda_{r,t}^{\mathrm{RG}}, \mu_{r,t}^{\mathrm{RG}}$ are dual variables corresponding to constraints of renewable generation (3.24), $\lambda_{m,t}^{\mathrm{CL}}, \mu_{m,t}^{\mathrm{CL}}$ are variables corresponding to constraints of critical loads (3.25), $\varrho_{r,t}^{\mathrm{RG}}$ and $\varrho_{m,t}^{\mathrm{CL}}$ are auxiliary variables that facilitate linearizing relative constraints. $\Gamma_r^{\mathrm{RG}} \in [0,1]$ and $\Gamma_m^{\mathrm{CL}} \in [0,1]$ are the uncertainty budgets that control the conservativeness of the model. The larger $\Gamma_r^{\mathrm{RG}}/\Gamma_m^{\mathrm{CL}}$ is, the more conservative the model will be.

2 MILP Reformulations

Let $f_{k,t}^{\mathrm{DS}}$ and $f_{k,t}^{\mathrm{DB}}$ respectively denote the revenue from supplying and purchasing electricity, where $f_{k,t}^{\mathrm{DS}} = p_{k,t}^{\mathrm{DS}} \times \alpha_{k,t}^{\mathrm{DS}}$, $f_{k,t}^{\mathrm{DB}} = p_{k,t}^{\mathrm{DB}} \times \alpha_{k,t}^{\mathrm{DB}}$. Let binary variables $v_{k,s,t}^{\mathrm{DS}}$ and $v_{k,l,t}^{\mathrm{DB}}$ respectively represent intersection points' locations on the residual supply/demand bidding curve. If $v_{k,s,t}^{\mathrm{DS}} = 1$,

it means that the supply offer curve intersects with the s^{th} segment of the residual demand curve. Similarly, if $v_{k,l,t}^{\mathrm{DB}} = 1$, it means that the demand bidding curve crosses the l^{th} segment of the residual supply curve. The two nonlinear terms $f_{k,t}^{\mathrm{DS}}$ and $f_{k,t}^{\mathrm{DB}}$ can be linearized by introducing an auxiliary binary parameter $\omega_{k,s,t}^{\mathrm{DS}}$. $\omega_{k,s,t}^{\mathrm{DS}} = 1$ means that this segment is horizontal, while $\omega_{k,s,t}^{\mathrm{DS}} = 0$ means that this segment is vertical. As described in previous sections, for each hour, the cleared bidding quota $p_{k,t}^{\mathrm{DS}}/p_{k,t}^{\mathrm{DB}}$ and the corresponding price $\alpha_{k,t}^{\mathrm{DS}}/\alpha_{k,t}^{\mathrm{DB}}$ are determined by intersection points between the NMGs' demand/supply bidding curves and the market residual supply/demand price-quota curves. When the intersection point locates on a vertical segment l ($v_{k,s,t}^{\mathrm{DS}} = 1, \omega_{k,s,t}^{\mathrm{DS}} = 0$), follow relationships can be observed:

$$p_{k,t}^{\mathrm{DS}} = \mathrm{P}_{k,s,t}^{\mathrm{DS,min}} v_{k,s,t}^{\mathrm{DS}} = \mathrm{P}_{k,s,t}^{\mathrm{DS,max}} v_{k,s,t}^{\mathrm{DS}} \tag{3.37}$$

$$\alpha_{k,t}^{\mathrm{DS}} = b_{k,s,t}^{\mathrm{DS}} + \alpha_{k,s,t}^{\mathrm{DS,min}} v_{k,s,t}^{\mathrm{DS}} \tag{3.38}$$

$$f_{k,t}^{\mathrm{DS}} = b_{k,s,t}^{\mathrm{DS}} \mathrm{P}_{k,s,t}^{\mathrm{DS,min}} + v_{k,s,t}^{\mathrm{DS}} \alpha_{k,s,t}^{\mathrm{DS,min}} \mathrm{P}_{k,s,t}^{\mathrm{DS,min}} \tag{3.39}$$

When the intersection point locates on a horizontal segment ($v_{k,s,t}^{\mathrm{DS}} = 1, \omega_{k,s,t}^{\mathrm{DS}} = 1$), follow relationships can be observed:

$$\alpha_{k,t}^{\mathrm{DS}} = \alpha_{k,s,t}^{\mathrm{DS,min}} v_{k,s,t}^{\mathrm{DS}} = \alpha_{k,s,t}^{\mathrm{DS,max}} v_{k,s,t}^{\mathrm{DS}} \tag{3.40}$$

$$p_{k,t}^{\mathrm{DS}} = a_{k,s,t}^{\mathrm{DS}} + \mathrm{P}_{k,s,t}^{\mathrm{DS,min}} v_{k,s,t}^{\mathrm{DS}} \tag{3.41}$$

$$f_{k,t}^{\mathrm{DS}} = a_{k,s,t}^{\mathrm{DS}} \alpha_{k,s,t}^{\mathrm{DS,min}} + v_{k,s,t}^{\mathrm{DS}} \alpha_{k,s,t}^{\mathrm{DS,min}} \mathrm{P}_{k,s,t}^{\mathrm{DS,min}} \tag{3.42}$$

In summary, $f_{k,t}^{\mathrm{DS}}$ can be linearized as:

$$\begin{aligned} f_{k,t}^{\mathrm{DS}} = \sum\nolimits_{s} \big[\big(b_{k,s,t}^{\mathrm{DS}} \mathrm{P}_{k,s,t}^{\mathrm{DS,min}} + v_{k,s,t}^{\mathrm{DS}} \alpha_{k,s,t}^{\mathrm{DS,min}} \mathrm{P}_{k,s,t}^{\mathrm{DS,min}} \big) \times \big(1 - \omega_{k,s,t}^{\mathrm{DS}} \big) \big] + [(a_{k,l,t}^{\mathrm{DS}} \alpha_{k,s,t}^{\mathrm{DS,min}} \\ + v_{k,s,t}^{\mathrm{DS}} \alpha_{k,s,t}^{\mathrm{DS,min}} \mathrm{P}_{k,s,t}^{\mathrm{DS,min}}) \times \omega_{k,s,t}^{\mathrm{DS}}] \end{aligned} \tag{3.43}$$

$$p_{k,t}^{\mathrm{DS}} = \sum\nolimits_{s} \big(\mathrm{P}_{k,s,t}^{\mathrm{DS,min}} v_{k,s,t}^{\mathrm{DS}} + a_{k,s,t}^{\mathrm{DS}} \big) \tag{3.44}$$

In addition, horizontal and vertical distances $a_{k,s,t}^{\mathrm{DS}}$ and $b_{k,s,t}^{\mathrm{DS}}$ between the intersection points and the endpoints of the segment are further limited by:

$$0 \le a_{k,s,t}^{\mathrm{DS}} \le v_{k,s,t}^{\mathrm{DS}}(\mathrm{P}_{k,s,t}^{\mathrm{DS,max}} - \mathrm{P}_{k,s,t}^{\mathrm{DS,min}}) \tag{3.45}$$

$$0 \le b_{k,s,t}^{\mathrm{DS}} \le v_{k,s,t}^{\mathrm{DS}}(\alpha_{k,s,t}^{\mathrm{DS,max}} - \alpha_{k,s,t}^{\mathrm{DS,min}}) \tag{3.46}$$

It can be observed from (3.43) that, if there is no intersection between the supply offer curve and the market residual demand curve ($v_{k,s,t}^{\mathrm{DS}} = 0$), then $f_{k,t}^{\mathrm{DS}} = 0$. If the intersection point locates on a horizontal segment, then $\mathrm{F}_{k,t}^{\mathrm{DS}}$ is calculated by (3.39). If it locates on a vertical segment, then $\mathrm{F}_{k,t}^{\mathrm{DS}}$ is calculated using (3.42).

Similarly, by introducing a binary parameter $\omega_{k,l,t}^{\mathrm{DB}}$, the revenue from purchasing electricity $f_{k,t}^{\mathrm{DB}}$ can also be linearized as follow:

$$\begin{aligned} f_{k,t}^{\mathrm{DB}} = \sum\nolimits_{l} & \left[\left(b_{k,l,t}^{\mathrm{DB}}\mathrm{P}_{k,l,t}^{\mathrm{DB,min}} + v_{k,l,t}^{\mathrm{DB}}\alpha_{k,l,t}^{\mathrm{DB,min}}\mathrm{P}_{k,l,t}^{\mathrm{DB,min}}\right) \times \left(1 - \omega_{k,l,t}^{\mathrm{DB}}\right)\right] \\ & + \left[\left(a_{k,l,t}^{\mathrm{DB}}\alpha_{k,l,t}^{\mathrm{DB,min}} + v_{k,l,t}^{\mathrm{DB}}\alpha_{k,l,t}^{\mathrm{DB,min}}\mathrm{P}_{k,l,t}^{\mathrm{DB,min}}\right) \times \omega_{k,l,t}^{\mathrm{DB}}\right] \end{aligned} \tag{3.47}$$

$$p_{k,t}^{\mathrm{DB}} = \sum\nolimits_{l}\left(\mathrm{P}_{k,l,t}^{\mathrm{DB,min}}v_{k,l,t}^{\mathrm{DB}} + a_{k,l,t}^{\mathrm{DB}}\right) \tag{3.48}$$

In addition, the horizontal and vertical distances between the intersection point and the endpoints of the intersected segment of residual supply price curves are further limited by:

$$0 \le a_{k,l,t}^{\mathrm{DB}} \le v_{k,l,t}^{\mathrm{DB}}(\mathrm{P}_{k,l,t}^{\mathrm{DB,max}} - \mathrm{P}_{k,l,t}^{\mathrm{DB,min}}) \tag{3.49}$$

$$0 \le b_{k,l,t}^{\mathrm{DB}} \le v_{k,l,t}^{\mathrm{DB}}(\alpha_{k,l,t}^{\mathrm{DB,max}} - \alpha_{k,l,t}^{\mathrm{DB,min}}) \tag{3.50}$$

Moreover, it is enforced by (3.51) and (3.52) that only one intersection point is allowed for each hour in each scenario, which physically means that the NMGs entity is prohibited from supplying and purchasing electricity simultaneously within the same time slot.

$$\sum\nolimits_{l} v_{k,l,t}^{\mathrm{DB}} = 1 - \theta_t \tag{3.51}$$

$$\sum_s v_{k,s,t}^{\mathrm{DS}} = \theta_t \tag{3.52}$$

After step 1&2, finally the MILP counterpart of the original model is presented conclusively as (3.53):

$$\max \sum_{k\in\Theta}^{\mathrm{K}} \varsigma_k \sum_{t=1}^{\mathrm{T}} \left(f_{k,t}^{\mathrm{DS}} - f_{k,t}^{\mathrm{DB}} - f_{k,t}^{OP}\right) \tag{3.53}$$

s.t. (3.1)-(3.23)&(3.27)-(3.36)&(3.43)-(3.52)

3.6.2 Dantzig-Wolfe Decomposition Method

In this chapter, the Dantzig-Wolfe Decomposition algorithm (DWD) is employed to solve the MILP counterpart of the bidding problem in a semi-decentralized manner. DWD is an efficient algorithm for solving large-scale MIP & LP. The iteration process of DWD is illustrated in Figure 3.3.

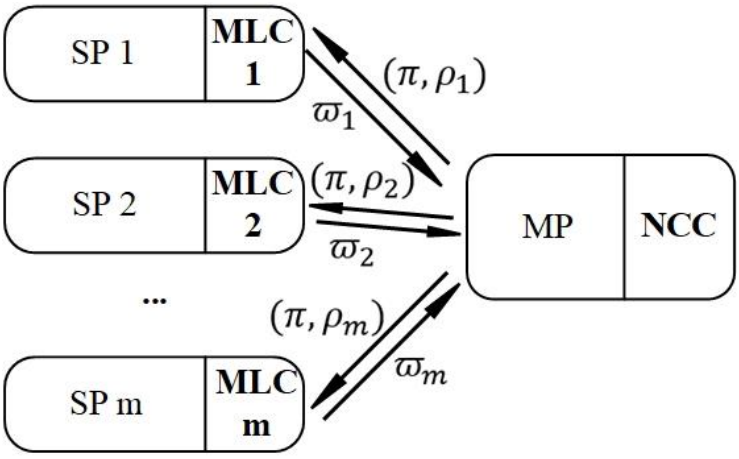

Figure 3.3 Illustration of Dantzig-Wolfe decomposition method

The DWD decomposes the MILP counterpart into a master problem (MP) and several pricing subproblems (SP). The MP subjects to the coupling constraints, including (3.20)&(3.22)&(3.23)&(3.27)-(3.30)&(3.43)-(3.52) and convexity constraints, and optimize public decision variables $X^P := [\theta_t\ p_{k,mj,t}^{\mathrm{INT}}\ f_{k,m,t}^{\mathrm{OP}}\ p_{k,m,t}^{\mathrm{NET}}\ p_{k,m,t}^{\mathrm{ES}}\ p_{k,m,t}^{\mathrm{EB}}\ v_{k,l,t}^{\mathrm{DB}}\ a_{k,l,t}^{\mathrm{DB}}\ b_{k,l,t}^{\mathrm{DB}}\ v_{k,s,t}^{\mathrm{DS}}\ a_{k,s,t}^{\mathrm{DS}}\ b_{k,s,t}^{\mathrm{DS}}]$. While the SP subjects to the independent constraints of each microgrid m, including (3.1)-

(3.19)&(3.21)&(3.32)-(3.36), and optimize local decision variables $X_m^{\mathrm{L}} \coloneqq [u_{k,g,t}^{\mathrm{CG}}\ p_{k,g,t}^{\mathrm{CG}}\ x_{k,e,t}^{\mathrm{ESS}}\ y_{k,e,t}^{\mathrm{ESS}}\ p_{k,e,t}^{\mathrm{Ch,ESS}}\ p_{k,e,t}^{\mathrm{Dis,ESS}}\ c_{k,e,t}^{\mathrm{ESS}}\ d_{k,m,t}^{\mathrm{DL}}\ p_{r,t}^{\mathrm{RG}}\ d_{m,t}^{\mathrm{CL}}]$. In each iteration, the NCC solves the MP and announces the dual variables corresponding to each coupling constraint(π, ρ_m) to each MLC, where while each MLC solves its corresponding pricing SP according to the received variables and returns generated columns ϖ_m to the MP, where integrality constraints can be enforced in this procedure. Optimum can be achieved by solving the MP and the SP iteratively. If the pricing SP does not return the columns with positive increase in the objective function, then the optimum is obtained. Details of the algorithm can be found in [94]–[96].

Privacy concerns of each microgrid can be eliminated by the DWD algorithm, as the NCC only has access to aggregated data or implicit non-physical-meaning data of each microgrid. In addition, advanced communication protocols have been proposed in some relevant studies to prevent the NCC from learning detail information of each MG [97]–[98].

3.7 Case Study

3.7.1 Test System Setups

The price-maker bidding model for NMGs developed in previous sections is used here to evaluate the potential net revenue of an NMGs cluster. The tested NMGs cluster is set up as shown in Table 3.1. This cluster consists of 9 fully-developed microgrids, which refers to the fact that each MG has the capability of operating in island mode at any time. Each MG has identical energy sources, including controllable generators, renewable generators, battery energy storage devices, critical loads and deferrable loads. Details of these energy sources are listed in Table 3.1.

Table 3.1 Setups of individual microgrids

		MG 1	MG 2	MG 3	MG 4	MG 5	MG 6	MG 7	MG 8	MG 9
CG	$\mathrm{P}_{g,\max}^{\mathrm{CG}}$	9	10	9	8	8	10	8	8	10
	$\mathrm{P}_{g,\min}^{\mathrm{CG}}$	1	2	1	1	2	2	2	1	1
	$\mathrm{R}_{g,\max}^{\mathrm{CG,U}}$	7.5	8.5	7.5	6.5	6.5	8.5	6.5	6.5	8.5
	$\mathrm{R}_{g,\max}^{\mathrm{CG,D}}$	6.5	6.5	6.5	5.5	4.5	6.5	4.5	5.5	7.5
	ϵ_g^{CG}	13	12	14	13	14	13	14	14	11

ESS	$SOC_{e,max}^{ESS}$ / $SOC_{e,min}^{ESS}$	0.9/0.1	0.9/0.1	0.95/0.05	0.9/0.1	0.9/0.1	0.9/0.1	0.95/0.05	0.9/0.1	0.9/0.1
	$C_{e,max}^{ESS}$	6	7	6	5	7	6	7	7	6
	$P_{e,max}^{Ch,ESS}$/ $P_{e,max}^{Dis,ESS}$	3	4	5	5	4	5	3	4	3
	$\eta_{e,c}^{ESS}$/ $\eta_{e,d}^{ESS}$	0.95/0.95	0.95/0.95	0.9/0.9	0.85/0.85	0.95/0.95	0.95/0.95	0.9/0.9	0.85/0.85	0.95/0.95
	$c_{e,0}^{ESS}$	3	2	3	2	2	3	2	3	2
	σ_e^{ESS}	12	12	12	12	12	12	12	12	12
DL	D_m^{DL}	3	2	2	3	3	2	2	3	3
	$D_{m,max}^{DL}$/ $D_{m,min}^{DL}$	0.8/0.2	0.9/0.1	0.9/0.1	0.9/0.1	0.8/0.2	0.9/0.1	0.9/0.1	0.9/0.1	0.8/0.2
	T_m^S/ T_m^E	10/18	0/7	0/7	20/24	10/18	0/7	0/7	20/24	10/18
RG	$P_r^{RG,max}$	4	5	3	4	4	5	3	4	4
CL	Peak load	15	15	14	14	15	14	15	14	15

In addition, there are multiple connection lines between individual microgrids, the interconnection status and corresponding transmission capacity are listed in Table 3.2. It should be noted that the diagonal elements refer to the transmission capacity between individual microgrids and the utility grid.

Table 3.2 Capacity limits on transmission lines between individual MGs

	MG1	MG2	MG3	MG4	MG5	MG6	MG7	MG8	MG9
MG1	12	5	–	–	–	–	–	–	6
MG2	5	10	–	3	1	4	–	–	–
MG3	–	–	13	4	–	–	0	2	–
MG4	–	3	4	9	–	–	4	–	4
MG5	–	1	–	0	12	3	–	3	–
MG6	–	4	–	0	3	10	1	3	–

MG7	–	–	–	4	–	1	10	–	3
MG8	–	–	2	–	3	3	–	12	3
MG9	6	–	–	4	–	–	3	3	11

In terms of the setups of uncertainty sources, those key parameters are set as Table 3.3. The central forecast values of renewable generation and critical load of individual MGs are both sampled according to the distribution of real measured data from the Alberta Electric System Operator (AESO).

While in terms of the market residual supply/demand curves, since the bidding problem is solved on a rolling time horizon basis, for each hour scheduling day, market residual supply/demand curves at the same hour of the past 10 days are used as the scenarios. These curves are built using data from the public database in [60]. It should be noted that the residual supply/demand curves are transformed into stepwise curves with the same number of steps for brevity.

Table 3.3 Setups of uncertainty parameters

Name	S	L	Θ	ς_k	Γ_r^{RG}	Γ_m^{CL}
Value	16	16	10	0.1	0.9	0.9

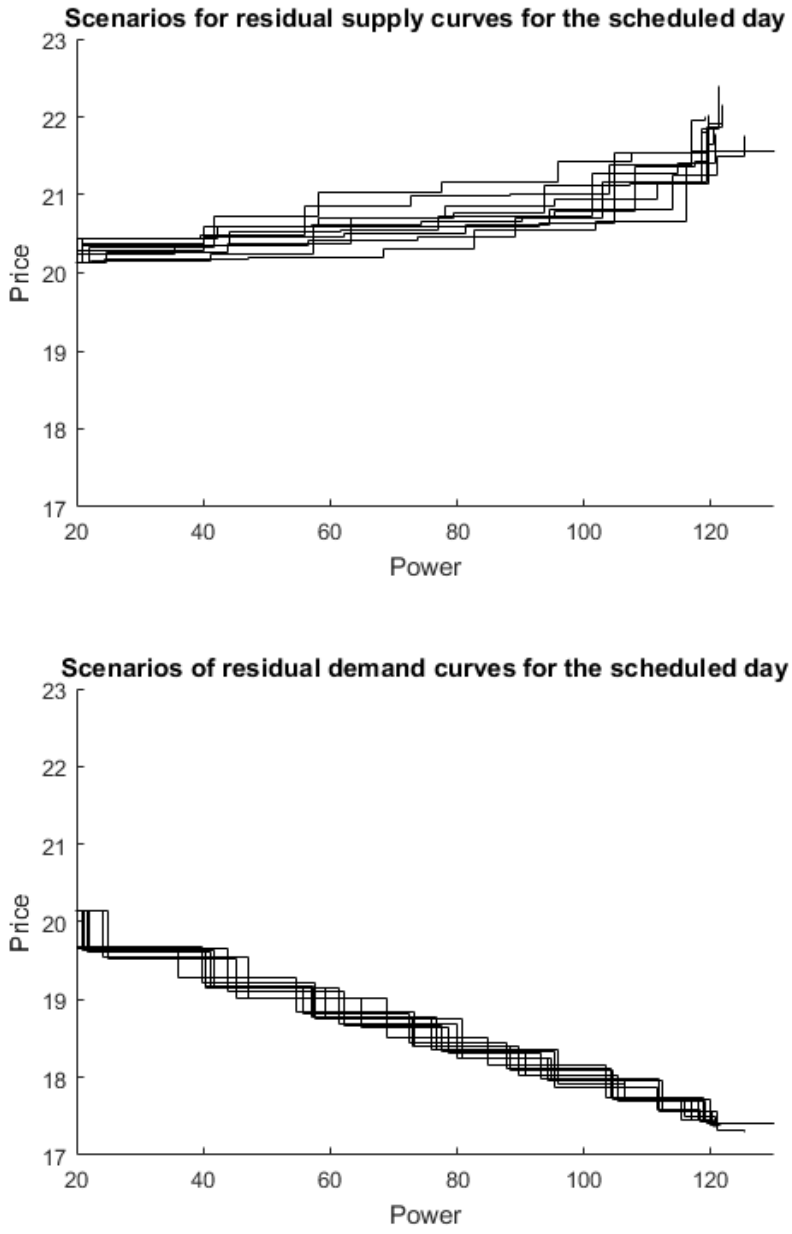

Figure 3.4 Scenarios of market residual supply/demand curves for the selected day

The numerical simulations are implemented on a desktop with an Intel i7-6700K CPU @ 3.40 GHz and 16.0 GB RAM memory. The market data is processed using MATLAB R2015b. The optimization model is implemented in GAMS 27.2.0. The CPLEX 12.8.0 is employed here as the solver.

3.7.2 Simulation Results

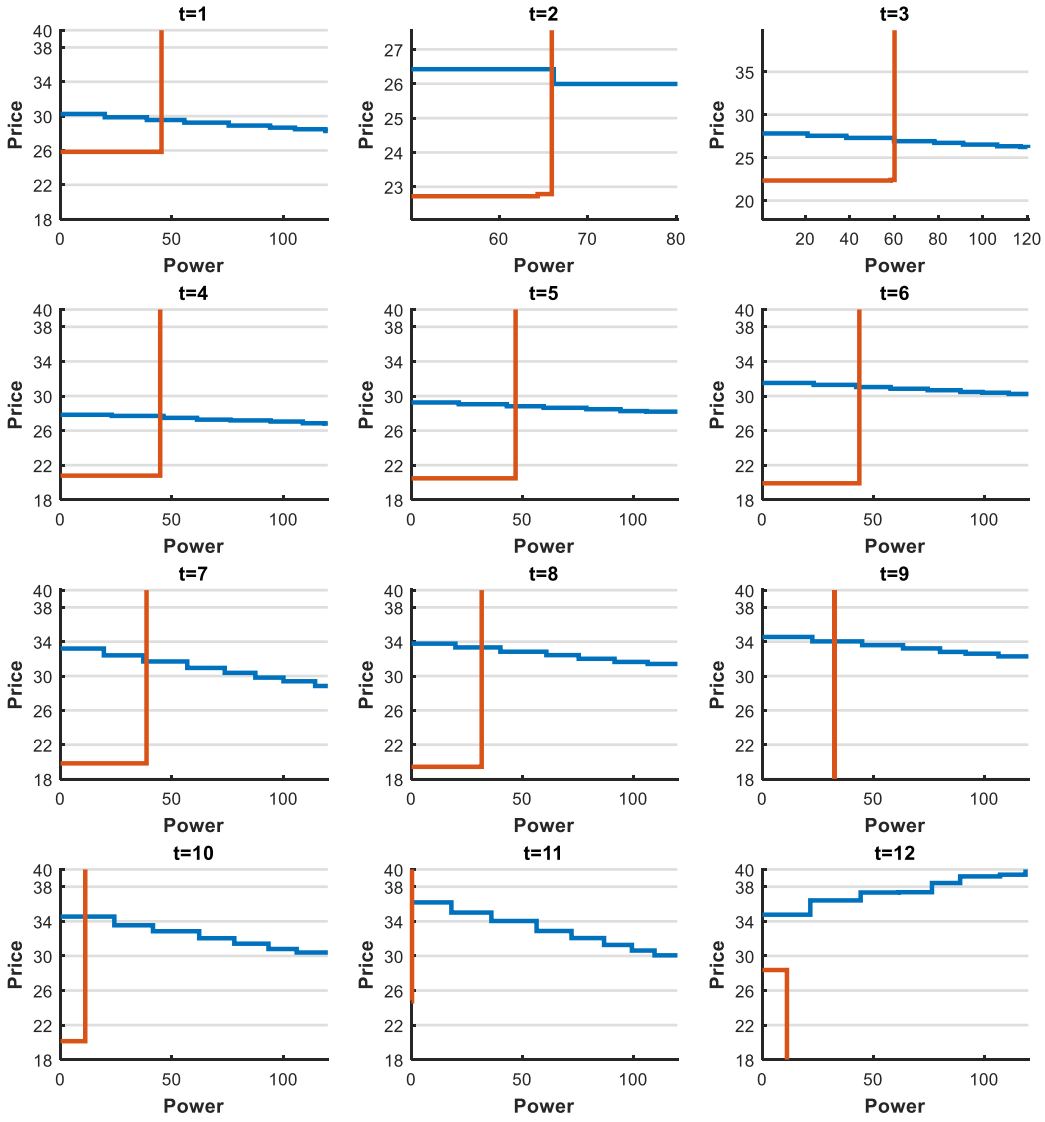

Figure 3.5 Scheduled price-quantity offers/bids from hour 1 to hour 12 with the corresponding market residual supply/demand curves

Firstly, the price-maker price-quantity curves for each hour of one selected scheduling day (Jan 26, 2018) are shown in Figure 3.5 and Figure 3.6. The power quantity and the corresponding price quantity of each hour are cleared at the intersection points between the submitted price-quantity offers/bids curves and the market residual supply/demand curves.

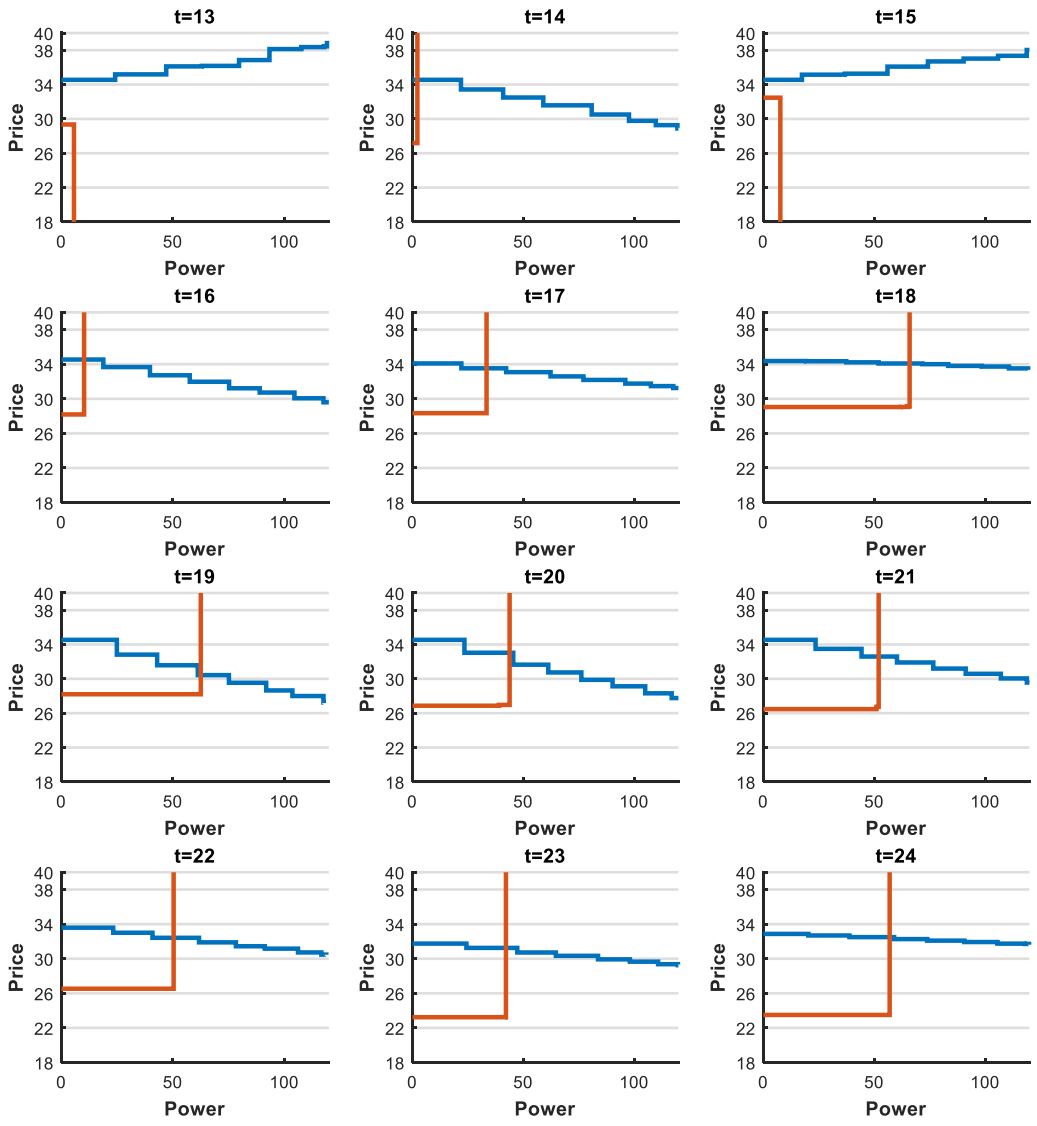

Figure 3.6 Scheduled price-quantity offers/bids for hour 13 to hour 24 with the corresponding market residual supply/demand curves

Next, the cleared price and power of price-taker bidding (PTB) strategy and price-maker bidding (PMB) strategy are compared. As shown in Figure 3.7, under the price-maker bidding strategy, the market price profiles become lower and smoother. However, when comparing the total net revenue obtained by the PMB and PTB, PMB ($ 25828.35) is higher than that of PTB ($ 24299.77), this is because that more power is cleared under the price-maker bidding strategy.

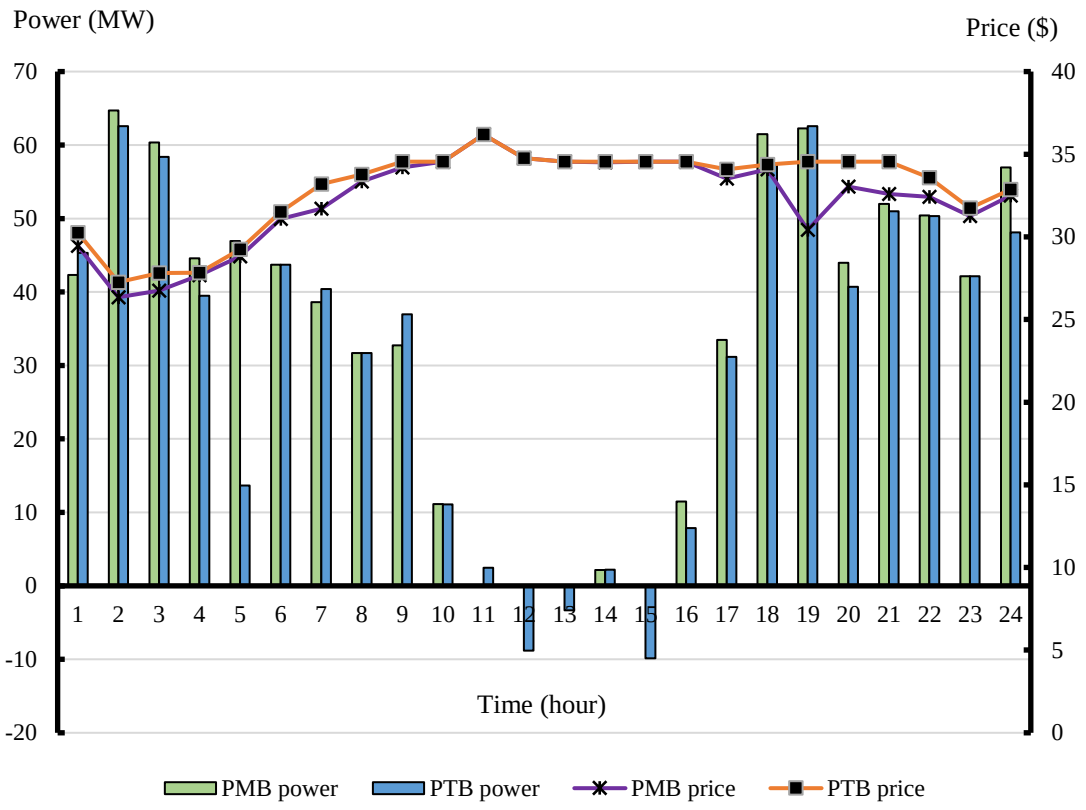

Figure 3.7 Comparison between price-taker and price-maker bidding strategy for the scheduled day

Finally, the monthly net revenue for the whole year 2018 is compared. Three different bidding strategies are considered here. The first one is the non-collaborative microgrids bidding strategy (NCMG), under which individual microgrids are not coordinated and do not have direct energy transactions with each other. Each microgrid participates solely in the pool based market as price-takers. The second one is the price-taker bidding strategy for networked microgrids, the NMGs submit offers/bids without the price quantity and takes whatever the market-clearing prices are, and the third one is the price-maker bidding strategy that has been proposed in previous sections. It can be found that: (1), comparing with non-collaborative bidding strategies, collaborative bidding strategies (including PTB & PMB) between individual microgrids will lead to higher net revenue, this is because that collaborations between microgrids will result in higher utilization level of energy storage devices and renewable generations; (2), comparing PTB and PMB bidding strategies, it can be found that PMB strategies will lead to higher net revenue. There is about 10% increase in annual net revenue compared with PTB strategies. The reason should be that, price-

maker bidding strategies create more potential intersection points in the market residual supply/demand curves, in addition, price-maker bidding strategies enable the NMGs to change the submitted power quantity as the market-clearing price changes.

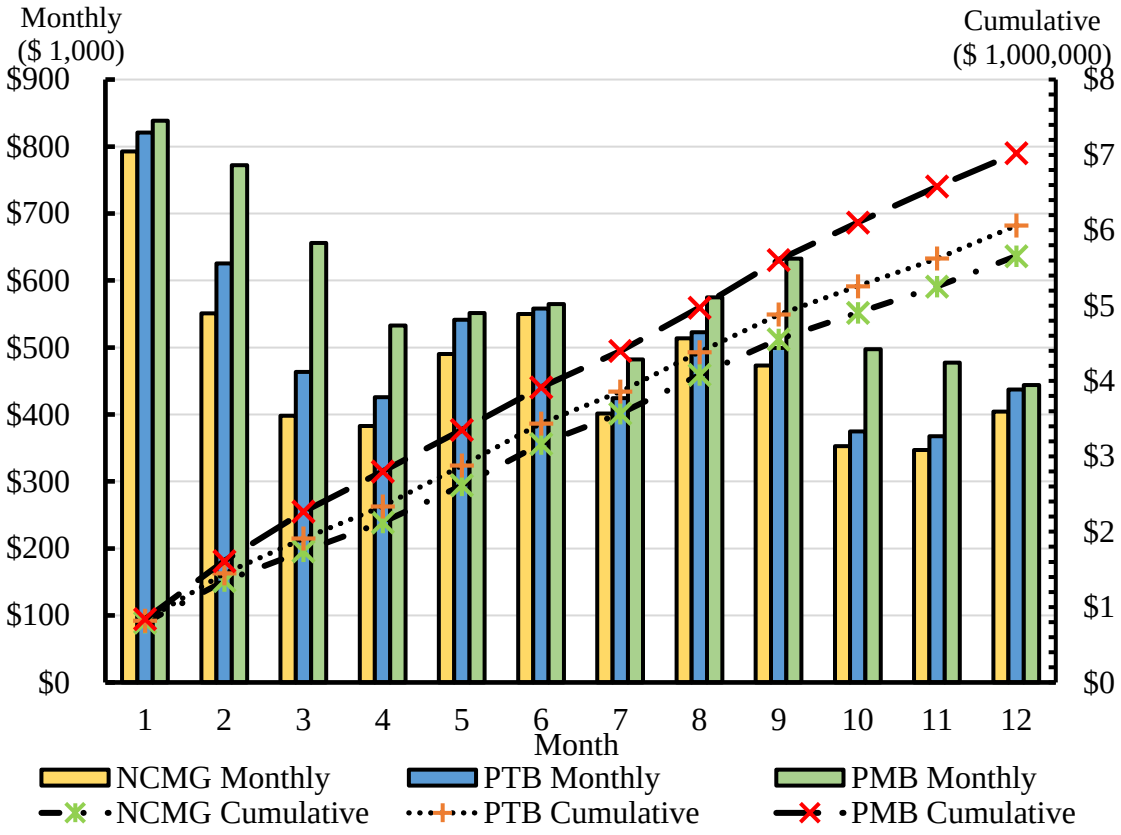

Figure 3.6 Monthly expected net revenue comparison between three different bidding strategies

3.8 Conclusion

This chapter presents a price-maker bidding model for NMGs in the day-ahead electricity market. This model aims at maximizing the NMGs' revenue by determining supply and demand bidding curves for each hour of the next day while subjecting to physical constraints of individual energy sources, interconnection lines, and market rules. The original hard-to-solve MINLP bidding problem is reformulated into its easy-to-solve MILP counterpart. The NMGs are coordinated under a semi-decentralized framework to protect the privacy of each microgrid as well as enhance the scalability of the bidding model. On the solution algorithms, in order to protect the privacy of

individual microgrids, the Dantzig-Wolfe decomposition (DWD) method is applied to solve the MILP counterpart to optimum in a semi-decentralized manner. Case studies are carried out based on real-world data. Results show that the proposed price-maker bidding strategy outperforms the existing price-taker bidding strategies in terms of expected total net revenue. Sensitivity analysis is conducted to investigate the impacts of different parameters on the objective function.

4 Conclusion and Future Work

4.1 Conclusions and Contributions

Microgrids are small, yet complex systems. The key components of a microgrid, including generator, energy management system, energy storage, and demand. The application of microgrid involves studies on electrical, control, economic and other aspects. In this thesis, studies on the system level modeling of microgrids have been carried out. The optimal bidding model for microgrids that seeks for maximizing the total net revenue in the context of deregulated pool-based electricity market is studied. The purpose of this research is to provide technical support to microgrid development on system-level to make microgrids a viable solution to the general public.

By promoting microgrids, people will become more open to microgrids. More research projects, practical applications, and investments can be attracted to contribute more to microgrids. The ultimate goal of this thesis is to fully excavate the potential of microgrids by tackling unsolved problems in the operation of microgrids. By providing solutions to such problem, not only the economic performances are improved, but also the negative environmental impact of human activities can be reduced.

In this chapter, the contributions of this thesis are summarized as follow:

- Microgrid system-level modeling and optimization. The key components of a microgrid are discussed and modeled in a computational trackable manner. In addition, the uncertainty sources in the system-level operation model are identified and mitigated using a hybrid stochastic-robust optimization framework, which can deliver robust and optimized solutions.
- Price maker bidding strategy for NMGs. Individual price-taker microgrids are coordinated to a price-maker NMGs entity that submits aggregated bids to the market. The overall economic performance is improved as the total net revenue expectation is increased. In addition, there is also improvement in the energy utilization level of each microgrid in the

NMGs, because physically interconnected microgrids are allowed to share electricity with each other.

- Coordination framework between individual microgrids. Considering that the ownership of individual microgrids may be different, the privacy concern becomes the major problem in the coordination framework. To obtain the global optimal while preserving each microgrid's privacy at the maximal level, the Dantzig-Wolfe decomposition method is employed to solve the coordination problem in a semi-decentralized manner. Only limited amount of privacy data is needed by the network central coordinator.

4.2 Future Work

As mentioned in former sections, the ultimate goal of our research is to deliver sound solutions to promote the development of microgrids. The frameworks and models in this thesis can be further improved in many aspects. Some possible suggestions to carry out future enhancements are listed as follow:

4.2.1 Real-Time Market Bidding Model

The main focus of this thesis is on the day-ahead bidding problem for a price-maker NMGs entity in the market. However, given the fact that almost all of the deregulated electricity markets are two-settlement markets, operation schedules for the NMGs in the intra-day horizon still needs more research.

4.2.2 Advanced Uncertainty Modeling Method

More advanced, sophisticated, yet computational trackable uncertainty modeling methods are needed to model the uncertainties of renewable generation and demand. In addition, microgrids generally are multi-carrier energy systems, which may consist of heating, cooling, gas, electricity, etc. Uncertainty management methods in future research should also consider the uncertainties of other forms of energy

4.2.3 Other Collaborations Among NMGs

Apart from providing energy service to the market, NMGs can also provide ancillary services to the market, including frequency regulation, voltage support, spinning and non-spinning reserve, and black start (system restoration), etc. By providing Microgrids' assets can be successfully leveraged to provide these services, and the total net revenue can be further maximized. However, in the context of providing ancillary services to the utility grid, the coordination between individual microgrids requires a more computational efficient solution method that can provide decisions in real-time.

4.2.4 Fair Porfit Allocation Method

It has been observed that the maximization in the total net profit does not necessarily mean the net profit of individual microgrids is maximized. So in the future a fair profit allocation method is needed to maximize the net profit of individual MGs and the whole NMGs entity simultaneously.

References

[1] R. W. Bacon and J. Besant-Jones, "Global electric power reform, privatization, and liberalization of the electric power industry in developing countries," *Annu. Rev. Energy Environ.*, vol. 26, pp. 331–359, Nov. 2001.

[2] T. Mai, D. Steinberg, J. Logan, D. Bielen, K. Eurek, and C. McMillan, "An electrified future: Initial scenarios and future research for U.S. Energy and electricity systems," *IEEE Power Energy Mag.*, vol. 16, no. 4, pp. 34–47, Jul. 2018.

[3] Dincer and Ibrahim, "Renewable energy and sustainable development: a crucial review," *Renew. Sustain. Energy Rev.*, vol. 4, no. 2, pp. 157–175, Jun. 2000.

[4] N. S. Pearre and L. G. Swan, "Renewable electricity and energy storage to permit retirement of coal-fired generators in Nova Scotia," *Sustain. Energy Technol. Assessments*, vol. 1, no. 1, pp. 44–53, Mar. 2013.

[5] A. K. Akella, "Geothermal Public Health Assessment," *FIG Congr. 2010*, vol. 34, no. 4, pp. 1–17, Apr. 2013.

[6] U. Lehr, C. Lutz, and D. Edler, "Green jobs? Economic impacts of renewable energy in Germany," *Energy Policy*, vol. 47, pp. 358–364, Aug. 2012.

[7] IRENA (2019), Renewable capacity statistics 2019, International Renewable Energy Agency (IRENA), Abu Dhabi.

[8] Global Additions in Distributed Generation Capacity to Increase Significantly. [Online]. Available: https://www.navigantresearch.com/news-and-views/global-additions-in-distributed-generation-capacity-to-increase-significantly.

[9] D. J. Ward, "Power quality and the security of electricity supply," *Proc. IEEE*, vol. 89, no. 12, pp. 1830–1836, Dec. 2001.

[10] C. Abbey *et al.*, "Powering through the storm: Microgrids operation for more efficient disaster recovery," *IEEE Power Energy Mag.*, vol. 12, no. 3, pp. 67–76, Apr. 2014.

[11] R. Viral and D. K. Khatod, “Optimal planning of distributed generation systems in distribution system: A review,” *Renewable and Sustainable Energy Reviews*, vol. 16, no. 7. pp. 5146–5165, Sep. 2012.

[12] L. I. Dulău, M. Abrudean, and D. Bică, “Effects of distributed generation on electric power systems,” *Procedia Technol.*, vol. 12, pp. 681–686, 2014.

[13] B. S. Hartono, Budiyanto, and R. Setiabudy, “Review of microgrid technology,” in *2013 International Conference on Quality in Research, QiR 2013 - In Conjunction with ICCS 2013: The 2nd International Conference on Civic Space*, pp. 127–132. Jun. 2013.

[14] Microgrids: Making way for customer control and renewable energy integration - MaRS Discovery District. [Online]. Available: https://www.marsdd.com/news/microgrids-making-way-for-customer-control-and-renewable-energy-integration/.

[15] *IEEE Std 2030.7-2017 : IEEE Standard for the Specification of Microgrid Controllers.* IEEE, 2018.

[16] The Advanced Microgrid: Integration and Interoperability (March 2014) | Department of Energy. [Online]. Available: https://www.energy.gov/oe/downloads/advanced-microgrid-integration-and-interoperability-march-2014.

[17] M. Barnes *et al.*, “Real-world microgrids–An overview,” in *2007 IEEE International Conference on System of Systems Engineering*, Apr. 2007.

[18] N. Hatziargyriou, H. Asano, R. Iravani, and C. Marnay, “Microgrids: An overview of ongoing research, development, and demonstration projects,” *IEEE Power & Energy Mag.*, issue 4, Aug. 2007.

[19] X. Zhong, L. Yu, R. Brooks, and G. K. Venayagamoorthy, “Cyber security in smart DC microgrid operations,” *2015 IEEE 1st International Conference on Direct Current Microgrids, ICDCM 2015*, pp. 86–91. Jun. 2015.

[20] P. Stluka, D. Godbole, and T. Samad, “Energy management for buildings and microgrids,” in *Proceedings of the IEEE Conference on Decision and Control*, pp. 5150–5157, Dec. 2011.

[21] J. Pascual, J. Barricarte, P. Sanchis, and L. Marroyo, “Energy management strategy for a

renewable-based residential microgrid with generation and demand forecasting," *Appl. Energy*, vol. 158, pp. 12–25, Nov. 2015.

[22] E. McKinney and J. Daniel Arjona, "Power utility-owned microgrids: A process for selecting scenarios for their implementation,"*2014 IEEE PES General Meeting | Conference & Exposition*, National Harbor, MD, 2014, pp. 1-5.

[23] New York Microgrids – Business Insider. [Online]. Available: https://www.businessinsider.com/new-york-microgrids-2016-6.

[24] C. Marnay, H. Asano, S. Papathanassiou, and G. Strbac, "Policymaking for microgrids," *IEEE Power Energy Mag.*, vol. 6, no. 3, pp. 66–77, May 2008.

[25] K. Milis, H. Peremans, and S. Van Passel, "The impact of policy on microgrid economics: A review," *Renewable and Sustainable Energy Reviews*, vol. 81. Elsevier Ltd, pp. 3111–3119, Jan. 2018.

[26] J. Wang, H. Zhong, W. Tang, R. Rajagopal, Q. Xia, C. Kang, Y. Wang., "Optimal bidding strategy for microgrids in joint energy and ancillary service markets considering flexible ramping products," *Appl. Energy*, vol. 205, pp. 294–303, Nov. 2017.

[27] C. Yuen and A. Oudalov, "The feasibility and profitability of ancillary services provision from multi-microgrids," *2007 IEEE Lausanne POWERTECH, Proc.*, pp. 598–603, Jul. 2007.

[28] A. Majzoobi, A. Khodaei, "Applications of microgrids in providing ancillary service to the utility grid," *Energy*, vol. 123, pp. 555-563, Mar. 2017.

[29] G. Liu, Y. Xu, and K. Tomsovic, "Bidding strategy for microgrid in day-ahead market based on hybrid stochastic/robust optimization," *IEEE Trans. Smart Grid*, vol. 7, no. 1, pp. 227–237, Jan. 2016.

[30] D. T. Nguyen and L. B. Le, "Optimal bidding strategy for microgrids considering renewable energy and building thermal dynamics," *IEEE Trans. Smart Grid*, vol. 5, no. 4, pp. 1608–1620, Jul. 2014.

[31] W. Tushar, T. K. Saha, C. Yuen, P. Liddell, R. Bean, and H. V. Poor, "Peer-to-peer energy

trading with sustainable user participation: A game theoretic approach," *IEEE Access*, vol. 6, pp. 62932–62943, Oct. 2018.

[32] A. Paudel, K. Chaudhari, C. Long, and H. B. Gooi, "Peer-to-peer energy trading in a prosumer-based community microgrid: A game-theoretic model," *IEEE Trans. Ind. Electron.*, vol. 66, no. 8, pp. 6087–6097, Aug. 2019.

[33] H. Khajeh, A. A. Foroud, and H. Firoozi, "Robust bidding strategies and scheduling of a price-maker microgrid aggregator participating in a pool-based electricity market," *IET Gener. Transm. Distrib.*, vol. 13, no. 4, pp. 468–477, Feb. 2019.

[34] AESO Market and system report . [Online]. Available: https://www.aeso.ca/market/market-and-system-reporting/.

[35] P. A. Ruiz, C. R. Philbrick, and P. W. Sauer, "Wind power day-ahead uncertainty management through stochastic unit commitment policies," *2009 IEEE/PES Power Systems Conference and Exposition*, Mar. 2009.

[36] W. van Ackooij, "A comparison of four approaches from stochastic programming for large-scale unit-commitment," *EURO J. Comput. Optim.*, vol. 5, no. 1–2, pp. 119–147, Mar. 2017.

[37] L. Zhao, B. Zeng, and B. Buckley, "A stochastic unit commitment model with cooling systems," *IEEE Trans. Power Syst.*, vol. 28, no. 1, pp. 211–218, May 2013.

[38] Q. P. Zheng, J. Wang, and A. L. Liu, "Stochastic optimization for unit commitment–A review," *IEEE Trans. Power Syst.*, vol. 30, no. 4, pp. 1913–1924, Jul. 2015.

[39] A. Papavasiliou and S. S. Oren, "Multiarea stochastic unit commitment for high wind penetration in a transmission constrained network," *Oper. Res.*, vol. 61, no. 3, pp. 578–592, May 2013.

[40] P. Carpentier, G. Cohen, and J. C. Culioli, "Stochastic optimization of unit commitment: A new decomposition framework," *IEEE Trans. Power Syst.*, vol. 11, no. 2, pp. 1067–1073, May 1996.

[41] S. Takriti, B. Krasenbrink, and L. S. Y. Wu, "Incorporating fuel constraints and electricity spot prices into the stochastic unit commitment problem," *Oper. Res.*, vol. 48, no. 2, pp.

268–280, Apr. 2000.

[42] S. Takriti, J. R. Birge, and E. Long, “A stochastic model for the unit commitment problem” *IEEE Trans. Power Syst.*, vol. 11, no. 3, pp. 1497–1508, Aug. 1996.

[43] R. Jiang, M. Zhang, G. Li, and Y. Guan, “Two-stage network constrained robust unit commitment problem,” *Eur. J. Oper. Res.*, vol. 234, no. 3, pp. 751–762, May 2014.

[44] A. Velloso, A. Street, D. Pozo, J. M. Arroyo, and N. G. Cobos, “Two-stage robust unit commitment for co-optimized electricity markets: An adaptive data-driven approach for scenario-based uncertainty sets,” *IEEE Trans. Sustain. Energy*, pp. 1–1, May 2019. doi: 10.1109/TSTE.2019.2915049

[45] W. Yuan, B. Zeng, E. Litvinov, T. Zheng, and J. Zhao, “Fast computing method for two-stage robust network constrained unit commitment problem,” in *IEEE Power and Energy Society General Meeting*, 2015, vol. Oct. 2015.

[46] A. Lorca, X. A. Sun, E. Litvinov, and T. Zheng, “Multistage adaptive robust optimization for the unit commitment problem,” *Oper. Res.*, vol. 64, no. 1, pp. 32–51, 2016.

[47] M. I. Alizadeh, M. P. Moghaddam, and N. Amjady, “Multistage multiresolution robust unit commitment with nondeterministic flexible ramp considering load and wind variabilities,” vol. 9, no. 2, pp. 872–883, Oct. 2017.

[48] A. Lorca and X. A. Sun, “Multistage Robust Unit Commitment with Dynamic Uncertainty Sets and Energy Storage,” *IEEE Trans. Power Syst.*, vol. 32, no. 3, pp. 1678–1688, May 2017.

[49] J. Goh and M. Sim, “Distributionally robust optimization and its tractable approximations,” *Oper. Res.*, vol. 58, no. 4 part 1, pp. 902–917, Jul. 2010.

[50] E. Delage and Y. Ye, “Distributionally robust optimization under moment uncertainty with application to data-driven problems,” *Oper. Res.*, vol. 58, no. 3, pp. 595–612, Jan. 2010.

[51] Y. Zhang, X. Han, M. Yang, B. Xu, Y. Zhao, and H. Zhai, “Adaptive robust unit commitment considering distributional uncertainty,” *Int. J. Electr. Power Energy Syst.*, vol. 104, no. 4, pp. 635–644, July 2018.

[52] C. Duan, L. Jiang, W. Fang, and J. Liu, "Data-driven affinely adjustable distributionally robust unit commitment," *IEEE Trans. Power Syst.*, vol. 33, no. 2, pp. 1385–1398, Aug. 2018.

[53] C. Ning and F. You, "Data-driven adaptive robust unit commitment under wind power uncertainty: A Bayesian nonparametric approach," *IEEE Trans. Power Syst.*, vol. 34, no. 3, pp. 2409–2418, Jan. 2019.

[54] Y. Chen, Q. Guo, H. Sun, Z. Li, W. Wu, and Z. Li, "A distributionally robust optimization model for unit commitment based on kullback-leibler divergence," *IEEE Trans. Power Syst.*, vol. 33, no. 5, pp. 5147–5160, Sept. 2018.

[55] P. Xiong and C. Singh, "A distributional interpretation of uncertainty sets in unit commitment under uncertain wind power," *IEEE Trans. Sustain. Energy*, vol. 10, no. 1, pp. 149–157, Jan. 2019.

[56] W. Wei, F. Liu, and S. Mei, "Distributionally robust co-optimization of energy and reserve dispatch," *IEEE Trans. Sustain. Energy*, vol. 7, no. 1, pp. 289–300, Jan. 2016.

[57] U. A. Ozturk, M. Mazumdar, and B. A. Norman, "A solution to the stochastic unit commitment problem using chance constrained programming," *IEEE Trans. Power Syst.*, vol. 19, no. 3, pp. 1589–1598, Aug. 2004.

[58] C. Zhao, Q. Wang, J. Wang, and Y. Guan, "Expected value and chance constrained stochastic unit commitment ensuring wind power utilization," *IEEE Trans. Power Syst.*, vol. 29, no. 6, pp. 2696–2705, Nov. 2014.

[59] W. Chen, M. Sim, J. Sun, and C. P. Teo, "From CVaR to uncertainty set: Implications in joint chance-constrained optimization," *Operations Research*, vol. 58, no. 2. pp. 470–485, Mar. 2010.

[60] California ISO Market Report. [Online]. Available: http://www.caiso.com/.

[61] J. P. Deane, G. Drayton, and B. P. Ó. Gallachóir, "The impact of sub-hourly modeling in power systems with significant levels of renewable generation," *Appl. Energy*, vol. 113, pp. 152–158, Jan. 2014.

[62] M. Carrión and J. M. Arroyo, “A computationally efficient mixed-integer linear formulation for the thermal unit commitment problem,” *IEEE Trans. Power Syst.*, vol. 21, no. 3, pp. 1371–1378, Jul. 2006.

[63] E. Ela and M. O'Malley, "Studying the Variability and Uncertainty Impacts of Variable Generation at Multiple Timescales," in *IEEE Trans. Power Syst.*, vol. 27, no. 3, pp. 1324-1333, Aug. 2012.

[64] G. Morales-españa, L. Ramírez-elizondo, and B. F. Hobbs, “Hidden power system inflexibilities imposed by traditional unit commitment formulations,” *Applied Energy*, vol. 191, pp. 223–238, Apr. 2017.

[65] Y. Wan and Y. Wan, “Analysis of wind power ramping behavior in ERCOT analysis of wind power ramping behavior in ERCOT,” *NREL Technical Report*, NREL/TP-5500-49218, Mar. 2011.

[66] M. Milligan and B. Kirby, “Analysis of Sub-Hourly Ramping Impacts of Wind Energy and Balancing Area Size,” *NREL Conference Paper*, NREL/CP-500-43434, Jun. 2008.

[67] Y. Dvorkin, D. S. Kirschen, and M. A. Ortega-vazquez, “Assessing flexibility requirements in power systems,” vol. 8, no. 4, pp. 1820–1830, Apr. 2014.

[68] ELIA Wind Generation Data. [Online]. Available: https://www.elia.be/en/grid-data/power-generation..

[69] R. Jiang, S. Member, J. Wang, Y. Guan, and A. Sets, “Robust Unit Commitment With Wind Power and Pumped Storage Hydro,” *IEEE Trans. Power Syst.*, vol. 27, no. 2, pp. 800–810, Nov. 2012.

[70] D. Bertsimas and M. Sim, “The Price of Robustness,” *Operations Research*, vol. 52, no.1, pp. 35-53, Jan. to Feb. 2004.

[71] B. Zeng and L. Zhao, “Solving two-stage robust optimization problems using a column-and- constraint generation method,” *Oper. Res. Lett.*, vol. 41, no. 5, pp. 457–461, Sep. 2013.

[72] M. Husein and I. Y. Chung, “Optimal design and financial feasibility of a university campus microgrid considering renewable energy incentives,” *Appl. Energy*, vol. 225, no. 5, pp. 273–

289, May 2018.

[73] W. Pei, Y. Du, W. Deng, K. Sheng, H. Xiao, and H. Qu, "Optimal bidding strategy and intramarket mechanism of microgrid aggregator in real-time balancing market," *IEEE Trans. Ind. Informatics*, vol. 12, no. 2, pp. 587–596, Jan. 2016.

[74] M. N. Alam, S. Chakrabarti, and A. Ghosh, "Networked microgrids: State-of-the-art and future perspectives," *IEEE Trans. Industrial Infomatics.*, vol. 15, no. 3, pp. 1238–1250, Nov. 2018.

[75] Z. Li, M. Shahidehpour, F. Aminifar, A. Alabdulwahab, and Y. Al-Turki, "Networked microgrids for enhancing the power system resilience," *Proc. IEEE*, vol. 105, no. 7, pp. 1289–1310, May 2017.

[76] X. Cao, J. Wang, J. Wang, and B. Zeng, "A risk-averse conic model for networked microgrids planning with reconfiguration and reorganizations," *IEEE Trans. Smart Grid*, pp. 1–1, Jul. 2019. doi: 10.1109/TSG.2019.2927833.

[77] K. Rahbar, C. C. Chai, and R. Zhang, "Energy cooperation optimization in microgrids with renewable energy integration," *IEEE Trans. Smart Grid*, vol. 9, no. 2, pp. 1482–1493, Aug. 2016.

[78] S. De La Torre, J. M. Arroyo, A. J. Conejo, and J. Contreras, "Price maker self-scheduling in a pool-based electricity market: A mixed-integer LP approach," *IEEE Trans. Power Syst.*, vol. 17, no. 4, pp. 1037–1042, Nov. 2002.

[79] M. Song and M. Amelin, "Price-maker bidding in day-ahead electricity market for a retailer with flexible demands," *IEEE Trans. Power Syst.*, vol. 33, no. 2, pp. 1948–1958, Feb. 2018.

[80] M. Kohansal and H. Mohsenian-Rad, "Price-maker economic bidding in two-settlement pool-based markets: The case of time-shiftable loads," *IEEE Trans. Power Syst.*, vol. 31, no. 1, pp. 695–705, Mar. 2016.

[81] Z. Wang, B. Chen, J. Wang, M. M. Begovic, and C. Chen, "Coordinated energy management of networked microgrids in distribution systems," *IEEE Trans. Smart Grid*, vol. 6, no. 1, pp. 45–53, Aug. 2015.

[82] G. E. Asimakopoulou, A. L. Dimeas, and N. D. Hatziargyriou, "Leader-follower strategies for energy management of multi-microgrids," *IEEE Trans. Smart Grid*, vol. 4, no. 4, pp. 1909–1916, May 2013.

[83] Z. Wang, B. Chen, J. Wang, and J. Kim, "Decentralized energy management system for networked microgrids in grid-connected and islanded modes," *IEEE Trans. Smart Grid*, vol. 7, no. 2, pp. 1097–1105, Jun. 2016.

[84] H. K. Nguyen, A. Khodaei, and Z. Han, "Incentive mechanism design for integrated microgrids in peak ramp minimization problem," *IEEE Trans. Smart Grid*, vol. 9, no. 6, pp. 5774–5785, Oct. 2018.

[85] W. Liu, J. Zhan, and C. Y. Chung, "A novel transactive energy control mechanism for collaborative networked microgrids," *IEEE Trans. Power Syst.*, vol. 34, no. 3, pp. 2048–2060, May 2019.

[86] H. Kim, J. Lee, S. Bahrami, and V. Wong, "Direct energy trading of microgrids in distribution energy market," *IEEE Trans. Power Syst.*, Jul. 2019. doi: 10.1109/TPWRS.2019.2926305.

[87] M. Fathi and H. Bevrani, "Statistical cooperative power dispatching in interconnected microgrids," *IEEE Trans. Sustain. Energy*, vol. 4, no. 3, pp. 586–593, 2013.

[88] D. Madjidian, M. Roozbehani, and M. A. Dahleh, "Energy storage from aggregate deferrable demand: Fundamental trade-offs and scheduling policies," *IEEE Trans. Power Syst.*, vol. 33, no. 4, pp. 3573–3586, 2018.

[89] PJM Market Report. [Online]. Available: http://www.pjm.com/.

[90] ERCOT Market Report. [Online]. Available: http://www.ercot.com/.

[91] G. Aneiros, J. M. Vilar, R. Cao, and A. Munõz San Roque, "Functional prediction for the residual demand in electricity spot markets," *IEEE Trans. Power Syst.*, vol. 28, no. 4, pp. 4201–4208, May 2013.

[92] H. Zhang, G. T. Heydt, V. Vittal, and J. Quintero, "An improved network model for transmission expansion planning considering reactive power and network losses," *IEEE*

Trans. Power Syst., vol. 28, no. 3, pp. 3471–3479, Apr. 2013.

[93] D. Bertsimas and M. Sim, "Robust discrete optimization and network flows," *Math. Program.*, vol. 98, no. 1–3, pp. 49–71, May 2003.

[94] J. Puchinger, P. J. Stuckey, M. G. Wallace, and S. Brand, "Dantzig-Wolfe decomposition and branch-and-price solving in G12," *Constraints*, vol. 16, no. 1, pp. 77–99, Jan. 2011.

[95] J. Desrosiers, "Branch-Price-and-Cut Algorithms," *In Wiley Encyclopedia of Operations Research and Management Science*, Jan. 2011. doi: 10.1002/9780470400531.eorms0118

[96] C. Barnhart, E. L. Johnson, G. L. Nemhauser, M. W. P. Savelsbergh, and P. H. Vance, "Branch-and-price: Column generation for solving huge integer programs," *Oper. Res.*, vol. 46, no. 3, pp. 316–329, May-Jun. 1998.

[97] Y. Hong, J. Vaidya, and H. Lu, "Secure and efficient distributed linear programming," *Journal of Computer Security*, vol. 20, pp. 583–634, Sep. 2012.

[98] J. E. Contreras-Ocaña, M. R. Sarker, and M. A. Ortega-Vazquez, "Decentralized coordination of a building manager and an electric vehicle aggregator," *IEEE Trans. Smart Grid*, vol. 9, no. 4, pp. 2625–2637, Oct. 2016.